Research Paper

GEOSPHERE

GEOSPHERE; v. 13, no. 2

doi:10.1130/GES01415.1

9 figures; 3 tables

CORRESPONDENCE: cronnevik@gmail.com

CITATION: Rønnevik, C., Ksienzyk, A.K., Fossen, H., and Jacobs, J., 2017, Thermal evolution and exhumation history of the Uncompahgre Plateau (northeastern Colorado Plateau), based on apatite fission track and (U-Th)-He thermochronology and zircon U-Pb dating: Geosphere, v. 13, no. 2, p. 518–537, doi:10.1130/GES01415.1.

Received 16 August 2016
Revision received 12 December 2016
Accepted 13 February 2017
Published online 17 March 2017

THE GEOLOGICAL SOCIETY OF AMERICA®

Thermal evolution and exhumation history of the Uncompahgre Plateau (northeastern Colorado Plateau), based on apatite fission track and (U-Th)-He thermochronology and zircon U-Pb dating

Christian Rønnevik[1], Anna K. Ksienzyk[1], Haakon Fossen[1,2], and Joachim Jacobs[1,3]

[1]Department of Earth Science, University of Bergen, PO Box 7803, 5020 Bergen, Norway
[2]University Museum of Bergen, PO Box 7800, 5020 Bergen, Norway
[3]Norwegian Polar Institute, Fram Centre, PO Box 6606 Langnes, 9296 Tromsø, Norway

ABSTRACT

Over the past two decades, thermochronological studies have greatly increased our knowledge of the Cenozoic evolution of the Colorado Plateau (western United States). There has been particular interest in the southwestern part of the plateau, leading to debate regarding the timing of uplift and fluvial incision along the Colorado River system. We here combine apatite fission track (AFT) and apatite (U-Th)-He (AHe) analyses as well as zircon U-Pb dating to investigate the much less studied northeastern Colorado Plateau, particularly the Uncompahgre Plateau and the Unaweep Canyon, which has a very unusual drainage pattern in two opposite directions.

We obtained 12 AFT ages from the Uncompahgre Plateau: 3 from the top of the basement of the plateau reveal Laramide ages (65–63 Ma), and 6 samples from the Unaweep Canyon (35–27 Ma) and 3 from the northeastern plateau margin (33–17 Ma) underwent complete thermal resetting in the late Eocene to Oligocene. Thermal history modeling of top basement samples reveals Late Cretaceous heating to temperatures of at least 90 °C, implying sedimentary burial to ~3 km, followed by cooling throughout the latest Cretaceous to Eocene. However, AHe ages (38–31 Ma) indicate minor reheating to 40–80 °C for these samples in the late Eocene to Oligocene.

Zircons from the La Sal Mountains laccolith gave an Oligocene U-Pb crystallization age of 29.1 ± 0.3 Ma. AFT ages from the laccolith range from 33 to 27 Ma, confirming rapid cooling of this shallow subvolcanic intrusion. This late Eocene to Oligocene magmatism caused thermal resetting of most of the AFT (except top basement) and AHe ages from the Uncompahgre Plateau, even though samples were collected as much as 60 km away from the intrusion. Canyon samples also underwent an increase in cooling rates in the past 5–10 m.y. This Miocene–Pliocene cooling event is interpreted as regional uplift of the Colorado Plateau associated with canyon incision.

INTRODUCTION

Although there is no doubt that the Colorado Plateau underwent Cenozoic uplift and erosion, the details in timing and magnitude of uplift are still poorly constrained. The Colorado Plateau was at sea level during the Late Cretaceous and was subsequently buried under several kilometers of marine sediments. Today, the average elevation of the Colorado Plateau is ~2 km. A fundamental problem in reconstructing the post-Cretaceous landscape evolution is that erosion has removed most of the Cenozoic sedimentary record on the Colorado Plateau.

Through various studies across western North America, both Cather et al. (2012) and Karlstrom et al. (2012) gave good overviews of the erosional history and recognized three main events of exhumation and tectonic uplift across the Colorado Plateau: (1) the Laramide orogeny (ca. 75–40 Ma) with differential basement-involved uplift limited to a few topographic highs, (2) mid-Cenozoic (ca. 35–15 Ma) erosion, primarily for the southwestern part of the Colorado Plateau, and (3) Neogene (10–6 Ma until present) uplift with considerably increased canyon incision across the entire plateau. How much the Laramide tectonism contributed to the overall uplift and how much should be attributed to Cenozoic epeirogenic events is still uncertain and the question of old versus young uplift with the subsequent erosional response, as well as the possible driving forces, are still debated topics (Karlstrom et al., 2012).

Thermochronological methods, especially low-temperature apatite fission track (AFT) and apatite (U-Th)-He (AHe) dating, are useful tools in this context, providing information about the cooling history of the upper crust within the temperature interval of 40–110 °C. They are ideally suited to investigate the Cenozoic history of the Colorado Plateau. However, care must be taken in evaluating these data, because the geothermal gradients might be strongly influenced by the presence of mid-Cenozoic magmatism (see distribution of volcanic rocks in Hunt, 1956; Roy et al., 2009; volcanic pattern in Nelson and Davidson, 1998) and later Neogene basaltic magmatism (e.g., van Wijk et al., 2010) within and along the plateau boundaries.

Numerous thermochronological studies have been applied to the southwestern part of the Colorado Plateau (e.g., Dumitru et al., 1994; Kelley et al., 2001; Flowers et al., 2008), and some data exist for the central parts (Stockli et al., 2002; Hoffman et al., 2011; Murray et al., 2016). Less attention has been devoted to the northeastern part of the plateau, including the Uncompahgre Plateau. Thomson et al. (2012) and Aslan et al. (2014) presented a few ages and models related to the highly debated origin of the Unaweep Canyon, which cuts across the Uncompahgre Plateau. In this paper we present new thermochronological data that help constrain the timing and magnitude of the Uncompahgre Plateau uplift. We also provide U-Pb zircon dates of the La Sal Mountains middle intrusive center, and together with existing thermochronological data we explore to what extent this magmatic event affected the cooling history of the northeastern part of the Colorado Plateau.

GEOLOGICAL SETTING

The Uncompahgre Plateau is a distinct topographic high within the larger Colorado Plateau region. It extends from the San Juan Mountains in southern Colorado in a northwestward direction until it plunges beneath the Uinta Basin in northeastern Utah (Figs. 1 and 2). The Uncompahgre Plateau is separated from the Paradox Basin on the southwest by steeply dipping reverse faults, and the overlying Mesozoic sediments have been flexed into faulted monoclines. Strata are nearly vertical along these structures, draped parallel to the steep fault planes that are interpreted as reverse faults at depth (e.g., Trudgill, 2011). The structures are interpreted as rejuvenated segments of an older fault system that formed during the late Paleozoic to early Mesozoic Ancestral Rocky Mountain orogeny (Cater, 1966, 1970; Case, 1991).

The eastern flank of the Uncompahgre Plateau is less well defined, because the northeastward-tilted plateau gently and uniformly dips beneath Quaternary deposits along the Gunnison River. However, some distinctive monoclines are present within the northeastern part of the plateau in the Colorado National Monument (CNM). These eroded monocline structures are exposed along the Monument, Fruita, and Redlands fault systems and are the results of high-angle faults within the Precambrian basement, most likely developed during Laramide contraction (Lohman, 1965; Jamison and Stearns, 1982; Jamison, 1989).

The Uncompahgre Plateau consists of Precambrian basement covered by a thick blanket of Mesozoic sedimentary rocks. While exposures of Precambrian rocks are generally scarce on the Colorado Plateau, good outcrops of early-Mesoproterozoic granitoids and gneissic rocks can be found within the deep canyons of the Uncompahgre Plateau (e.g., Case, 1991), particularly the Unaweep Canyon (Figs. 2A, 2B). This distinctive canyon cuts across the plateau in a southwest-northeast direction and provides an excellent cross section of the basement. A well-defined unconformity between the basement and upper Triassic red siltstone is evident. Subsequent depositions on the plateau are Triassic–Jurassic sandstones and siltstones, followed by alternating Cretaceous shales and sandstones. The youngest sediments still preserved today are remnants of the Cenomanian–Campanian Dakota Sandstone and Mancos Shale (e.g., Williams, 1964; Jamison and Stearns, 1982). A latest Cretaceous–Cenozoic sedimentary record is missing on the Uncompahgre Plateau. In the nearby Book Cliffs, however, the preserved sedimentary section includes the younger Cretaceous part of the Mesaverde Group

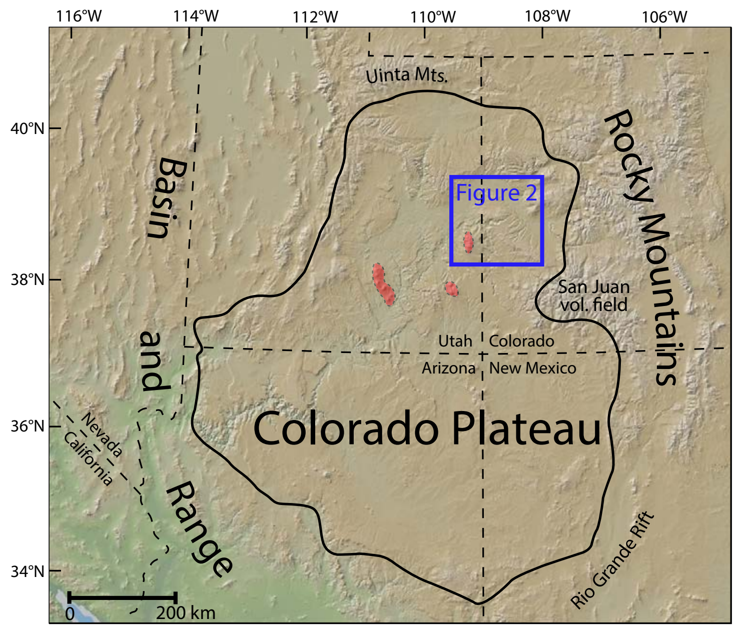

Figure 1. Digital elevation model of the Colorado Plateau and surrounding tectonic provinces. The blue square shows the field area. Red shading marks the laccolith complexes found within the plateau. Mts.—mountains; vol.—volcanic.

and Paleocene to Eocene Wasatch and Green River Formations (Williams, 1964; Gualtieri, 1988). Whether the missing section was never deposited on the Uncompahgre Plateau or has been removed by later erosion during one or several periods of Laramide or younger tectonic uplift and exhumation is still debated.

A striking feature of the northern Uncompahgre Plateau is the Unaweep Canyon, which, somewhat mysteriously, is drained by two creeks (Fig. 3) flowing in opposite directions from a gentle topographic divide at 2150 m within the canyon. This unusual drainage pattern has received a lot of attention since it was first described in the late 1800s (Peale, 1877; Gannett, 1882); the most recent contributions are Aslan et al. (2014) and Soreghan et al. (2015). Most observers agree that these creeks cannot alone be responsible for the incision of the Unaweep Canyon. A graben structure (Ute Creek graben; Fig. 2A) intersects the western creek. Soreghan et al. (2015) summarized the three main hypotheses for the formation of the canyon.

1. The prevailing hypothesis seems to be that the canyon originates from late Cenozoic fluvial erosion by the ancestral Gunnison River (e.g., Peale, 1877; Cater, 1966; Sinnock, 1981; Kaplan et al., 2005; Soreghan et al., 2015) and/or Colorado River (e.g., Gannett, 1882; Hunt, 1956; Lohman, 1961, 1965, 1981; Aslan et al., 2008, 2014; Hood, 2011; Hood et al., 2014), which later abandoned

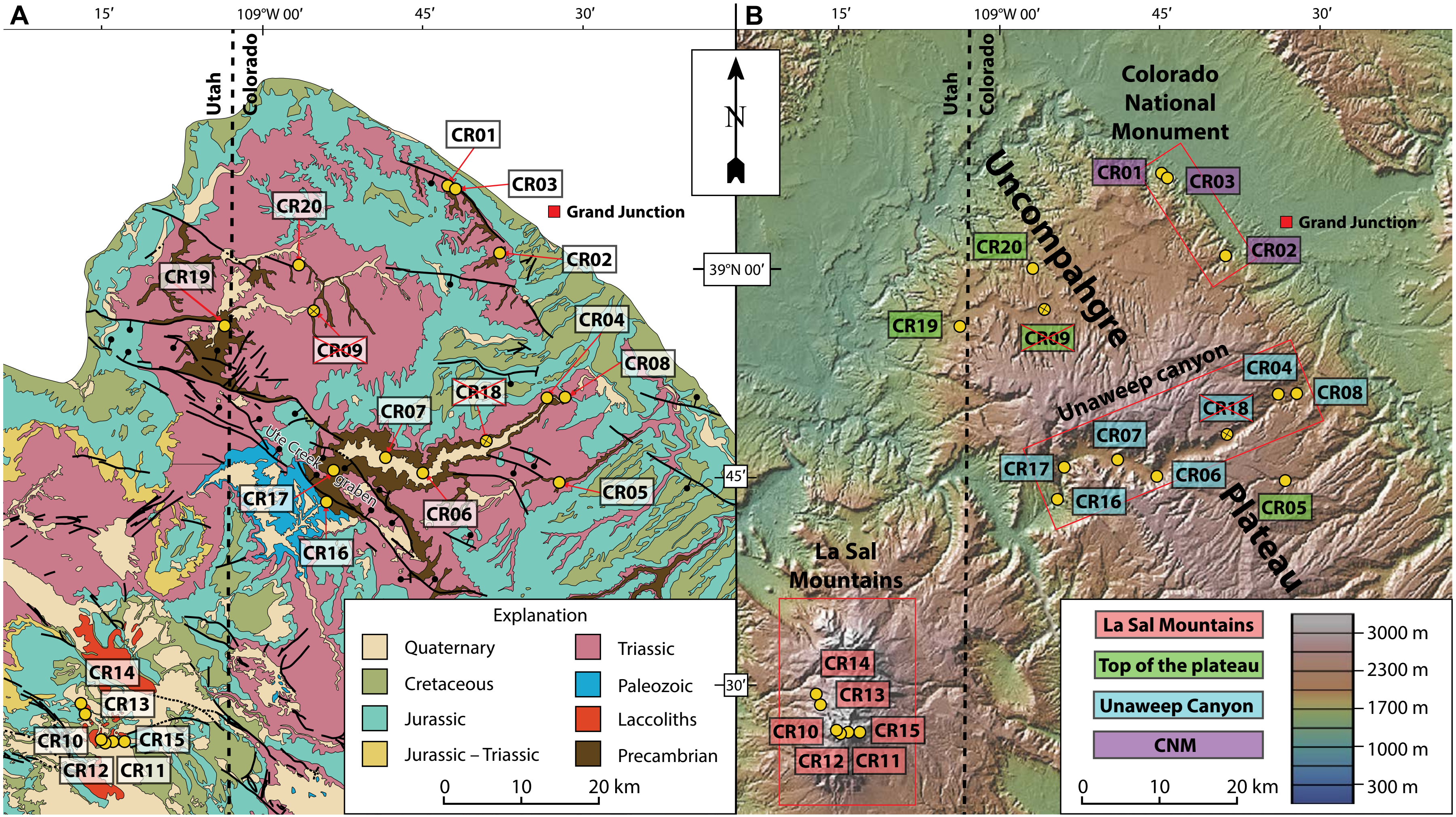

Figure 2. (A) Simplified geological map of the field area, based on Williams (1964) and Cashion (1973). (B) Topography of the field area, showing sample locations and geographical groups. Crossed-out samples did not yield enough apatite for apatite fission track (AFT) analysis. CNM—Colorado National Monument.

the canyon to move to their current river beds. The height and unusual location of the Unaweep drainage divide have led researchers to believe that this abandonment may have been caused by relatively recent tectonic uplift of the Uncompahgre Plateau (e.g., Lohman, 1965; Cater, 1966; Sinnock, 1981; Scott et al., 2002). However, despite a few younger Quaternary fault movements reported south of the canyon (Kirkham and Rogers, 1981; McCalpin, 2004, 2006), there is no clear structural evidence supporting such a neotectonic uplift event.

2. An alternative explanation is a late Cenozoic (Pleistocene) glacial incision of the canyon. This was inspired by the seemingly U-shaped profile of the Unaweep Canyon (e.g., Lohman, 1981; Cole and Young, 1983). Based on glacial features of the inner gorge cut into the Precambrian basement, Cole and Young (1983) suggested a possible late Pleistocene alpine glaciation. However, a geophysical survey showed that the bedrock profile is most likely V-shaped, and that the modern U-shape can be attributed to valley-fill sedimentation (Oesleby, 1983, 2005).

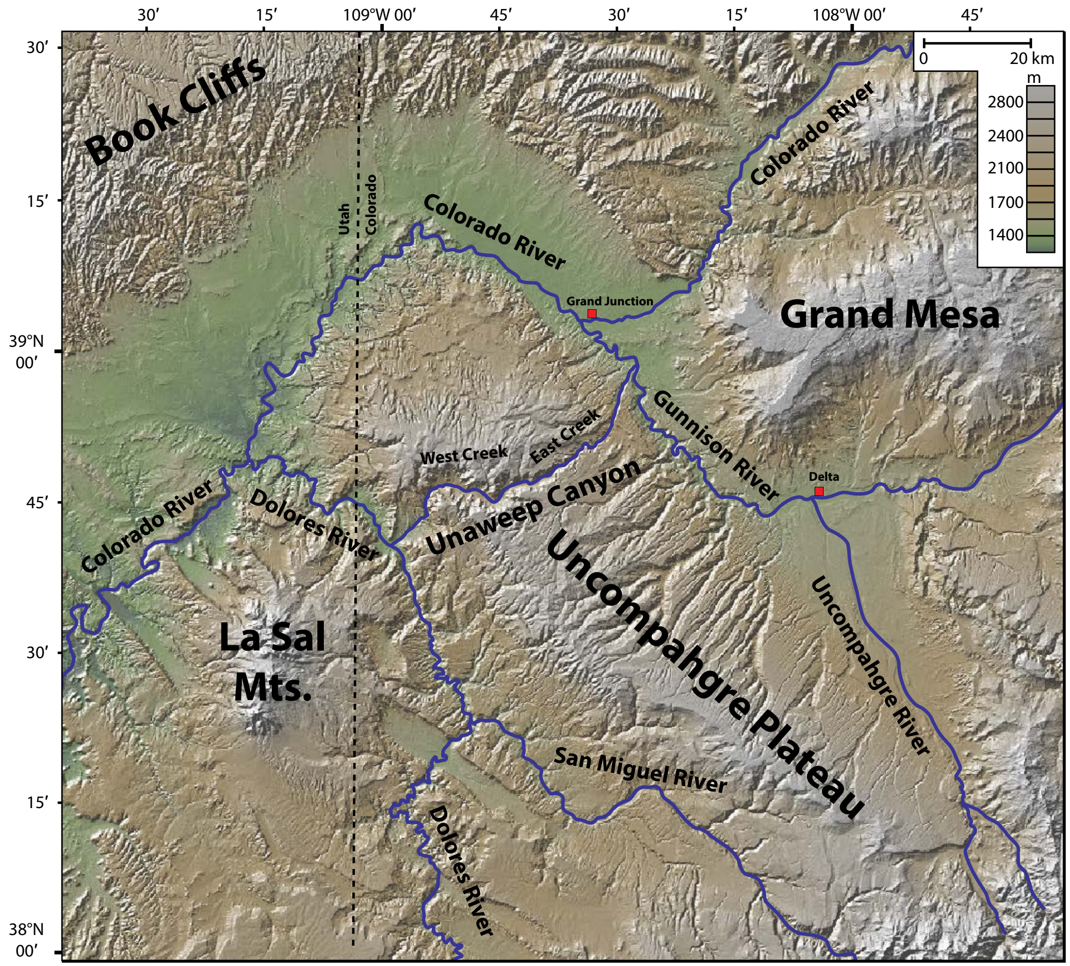

Figure 3. Topographic map of the Uncompahgre Plateau and the surrounding sedimentary and volcanic features (Book Cliffs, Grand Mesa, and La Sal Mountains), illustrating the area drainage pattern. Mts.—mountains.

3. The discovery of some late Paleozoic palynomorphs in drilled sedimentary strata close to the bedrock contact led Soreghan et al. (2007) to interpret the canyon as an exhumed late Paleozoic glacial landform, shaped by the Permian–Pennsylvanian glaciation during the ancient Uncompahgre uplift (Ancestral Rocky Mountains), rapidly buried by late Cenozoic fluvial processes and finally re-exhumed (Soreghan et al., 2008, 2014, 2015). However, this hypothesis is rather controversial: the low latitude and low elevation (near sea level) position of a potential Permian glacier, the current valley shape (V-shaped profile in the eastern part), Quaternary pollen that occur together with the Paleozoic palynomorphs, and suggested reworking of Paleozoic diamictites, as well as an absence of thickening of Mesozoic strata toward the canyon, all cast doubt on this interpretation (Hood, 2009; Hood et al., 2009; Soreghan et al., 2009a, 2009b).

Immediately to the west of the Uncompaghre Plateau are the shallow intrusions of the La Sal Mountains, which form one of several Paleogene laccolithic complexes within the Colorado Plateau. Whereas Cenozoic volcanic centers are mostly located along the plateau boundaries, these classical laccolithic intrusions are located within more central parts of the plateau (Fig. 1), notably the La Sal, Abajo, and the Henry Mountains (e.g., Hunt, 1956). The La Sal Mountains, just 30–40 km west of the Uncompahgre Plateau, include 3 of the 15 laccolith clusters of the Colorado Plateau, emplaced at levels ranging between 1.9 and 6.0 km (Ross, 1998).

Previous Age Determinations

The age of the La Sal Mountains laccoliths was determined by U-Pb zircon dating to be 32 ± 2 Ma (Stern et al., 1965); however, this age was obtained using the borax fusion technique, which dissolves the entire zircon grain, including possibly present and much older inherited cores. Later attempts were made utilizing the hornblende, augite, and biotite K-Ar (28–23 Ma), hornblende and feldspar ^{40}Ar-^{39}Ar (28–25 Ma), and AFT (31–29 Ma) methods (Stern et al., 1965; Armstrong, 1969; Sullivan et al., 1991; Nelson et al., 1992; Chew and Donelick, 2012). Similar ages are also found within other laccolithic intrusions of the Henry and Abajo Mountains (Sullivan et al., 1991; Nelson et al., 1992). Some older, Paleocene–Eocene hornblende K-Ar ages of 63–41 Ma from all three intrusions have been interpreted as the result of incompletely outgassed xenocrysts and excess of ^{40}Ar in hornblende (Nelson et al., 1992).

Two thermochronological studies have been carried out in the Unaweep Canyon. Thomson et al. (2012) reported AFT ages of 25–20 Ma and zircon fission track ages of 390–280 Ma from the southwestern part of the canyon. Three AHe ages of 25–17 Ma and another age of 42 Ma were reported for the central part of the canyon, while two ages of 23 and 47 Ma were given for the southwestern part. A few zircon (U-Th)-He ages were also reported, but show a wide scatter, 309–34 Ma. Thermal history models of their AFT data suggest complete thermal resetting of the AFT system in the late Eocene to Oligocene and two periods of rapid cooling, the first in the late Oligocene–early Miocene and the second during the last 6–10 m.y. A recent study by Aslan et al. (2014) includes two AFT ages: a younger age of 22 Ma from the southwestern part of the canyon and an older age of 38 Ma from the northeastern part. Based on thermal history modeling for these two samples, Aslan et al. (2014) suggested three pulses of cooling, one at 45–40 Ma, another at 30–25 Ma, and a pulse with more accelerated cooling during the past 10 m.y. Aslan et al. (2014) linked the first pulse to post-Laramide exhumation that supposedly began in Eocene to Oligocene time; they linked the second pulse to the relaxation of isotherms following magmatism in the San Juan volcanic field. Aslan et al. (2014) provided no explanation for the late Miocene–recent cooling pulse, but Thomson et al. (2012) interpreted this final cooling as canyon incision, because the signal is most pronounced in samples from low elevations within the canyon.

SAMPLES AND METHODS

We collected 20 samples in this study; 14 of these were taken from the Precambrian basement of the Uncompahgre Plateau, and the other 6 are from the middle laccolithic intrusion of the La Sal Mountains (Figs. 2A, 2B). Samples collected from the Uncompahgre Plateau can be divided into three groups: (1) seven samples from within the Unaweep Canyon, which cuts deeply into the basement rocks, (2) four samples away from the canyon close to the top of the basement, just below the overlying sediments, and (3) three samples from the northeastern plateau margin in the CNM. Apatite and zircon separates were obtained using conventional magnetic and heavy liquid separation techniques; 18 samples yielded enough apatite and were analyzed by the AFT method. Two samples from the Uncompahgre Plateau were also selected for AHe analysis and one sample from the La Sal Mountains was selected for U-Pb zircon dating.

AFT Analysis

AFT analyses were carried out at the Department of Earth Science, University of Bergen (Norway), using the external detector method (e.g., Donelick et al., 2005). The apatites were embedded in epoxy and then ground and polished to reveal internal crystal surfaces. Prior to irradiation, the apatites were etched in 5M HNO_3 for 20 ± 0.5 s at a temperature of 20 ± 1 °C. Each sample was then covered with a mica detector. The samples were irradiated together with Durango and Fish Canyon Tuff age standards and four IRMM-540R glasses (15 ppm U; distributed evenly throughout the sample stack) at the FRM II Forschungs-Neutronenquelle, Technical University of Munich. The mica detectors were subsequently etched at room temperate in 40% HF for 20 min. Spontaneous and induced fission tracks were counted using an optical microscope with a magnification of 1250×. A kinetic stage was used to control the grain to mica matching (Dumitru, 1993). Central fission track ages were calculated with the TrackKey software (Dunkl, 2002), using the zeta calibration method (Hurford and Green, 1983). Track length and etch pit measurements were performed at 2000× magnification. Due to relatively low track densities, eight samples were irradiated with ^{252}Cf to increase the number of etchable confined tracks.

AHe Analysis

AHe analyses were carried out at the Geoscience Centre, University of Göttingen (Germany). Single apatite crystals were hand-picked using binocular and petrographic microscopes. Only euhedral grains with two terminations were selected, and the length and width of each crystal were recorded. To determine the ^{4}He content, each individual grain was packed in a platinum capsule and the capsule with the enclosed crystal was degassed under high vacuum by heating with an infrared diode laser. After purification with a SAES Ti-Zr getter at 450 °C, the extracted gas was analyzed with a Hiden triple-filter quadrupole mass spectrometer, equipped with a positive ion counting detector. To ascertain a quantitative helium extraction, re-extraction was performed for every sample.

To analyze the ^{238}U, ^{232}Th, and Sm contents, the platinum capsules were retrieved after He analysis and the apatites were dissolved in nitric acid. The dissolved crystals were spiked with calibrated ^{230}Th and ^{233}U solutions and analyzed by the isotope dilution method on a Perkin Elmer Elan DRC inductively coupled–mass spectrometer equipped with an APEX microflow nebulizer. Form-dependent alpha-ejection corrections (F_T corrections) were applied to all raw AHe ages, following the procedures of Farley et al. (1996) and Hourigan et al. (2005).

U-Pb Zircon

U-Pb zircon dating was carried out at IBERSIMS (SHRIMP Ion-Microprobe Laboratory, University of Granada, Spain). Zircons were hand-picked and embedded in an epoxy mount, together with grains of the TEMORA-1 standard, the SL13 standard and the REG zircon. The mount was then ground to approximately half the grain thickness and polished, and the zircons were documented by optical (reflected and transmitted light) and scanning electron microscopy (secondary electrons and cathodoluminescence). Prior to analysis, the mount was coated with 8–10 nm of ultrapure gold. The analytical method follows that in Williams and Claesson (1987). Each spot was rastered with the primary beam for 120 s and then analyzed during 6 scans following the isotope peak sequence $^{196}Zr_2O$, ^{204}Pb, $^{204.1}$background, ^{206}Pb, ^{207}Pb, ^{208}Pb, ^{238}U, ^{248}ThO, ^{254}UO. Every peak of every scan was measured sequentially 10 times with the following total counting times per scan: 2 s for mass 196; 5 s for masses 238, 248, and 254; 15 s for masses 204, 206, and 208; and 20 s for mass 207. The primary beam was set to an intensity of ~5 nA, with a 120 μm Kohler aperture, which generates 17 × 20 μm elliptical spots on the target. The secondary beam exit slit was fixed at 80 μm, achieving a resolution of ~5000 at 1% peak height. The following calibrations were carried out: (1) mass calibration using the REG zircon (ca. 2.5 Ga, very high U, Th, and common lead content), (2) U-concentration using the SL13 zircon (238 ppm U; Claoue-Long et al., 1995), and (3) isotope ratios using the TEMORA-1 standard (416.8 ± 1.1 Ma; Black et al., 2003). Data reduction was performed with the SHRIMPTOOLS software v. 5.0 (developed by Fernando Bea for IBERSIMS, http://www.ugr.es/~fbea/fbea/Software.html). Errors are given at a 1σ level. The $^{206}Pb/^{238}U$ ratio is calculated from the measured $^{206}Pb^+/^{238}U^+$ and UO^+/U^+ following the method described by Williams (1998). For high-U zircons (U > 2500 ppm), $^{206}Pb/^{238}U$ is further corrected using the algorithm of Williams and Hergt (2000).

RESULTS AND INTERPRETATIONS

U-Pb Zircon Dating

Zircons from sample CR15 from the middle La Sal Mountains laccolith were U-Pb dated by SHRIMP (sensitive high-resolution ion microprobe) to obtain a precise crystallization age for the intrusion. Most zircons show well-defined euhedral shapes with length:width ratios between 2:1 and 4:1. Internally, the zircons are dominated by oscillatory zoned domains (Fig. 4), interpreted as magmatic zircon growth. Some zircons have no detectable cores (Fig. 4A) or only small euhedral cores that are concordant to the surrounding oscillatory domains and most likely grew during the same magmatic episode (Fig. 4B). Many zircons, however, show clear core-rim relationships, with more complex and often diffuse zoning in the cores (Fig. 4C). These cores generally appear to be rounded fragments of larger grains and are interpreted to be xenocrystic cores inherited from the source region of the melts.

We analyzed 31 spots on 27 grains (Table 1); 22 spots were located on oscillatory-zoned domains, 3 spots were on assumedly magmatic cores, and 6 were on xenocrystic cores. The data were filtered for quality, and two ages, both for magmatic cores, with a discordance >10% and/or 1σ error >5%, were excluded. The six xenocrystic cores yielded $^{207}Pb/^{206}Pb$ ages between ca. 1760 and 1660 Ma and are consistent with derivation of the magmas from the Paleoproterozoic crust underlying the field area. The older of these zircon core ages are typical for the Yavapai province and have crystallization ages of 1.8–1.7 Ga (e.g., Shawe and Karlstrom, 1999; Whitmeyer and Karlstrom, 2007); the youngest zircon cores suggest a Mazatzal-type origin (1.7–1.6 Ga). However, large 1720–1670 Ma plutons also occur within the Yavapai prov-

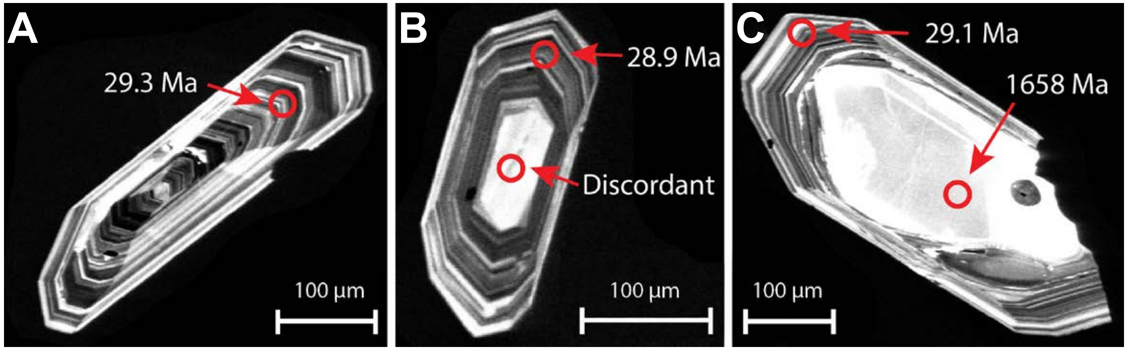

Figure 4. Three different types of zircons from sample CR15. All grains show finely laminated oscillatory zoned domains, interpreted to be of magmatic origin. (A) Zircon represents an example of a grain without a core. (B) Zircon has a small euhedral core thought to be cogenetic with the oscillatory zoned mantle (gave a Cenozoic but highly discordant age). (C) Zircon has a rounded, xenocrystic core.

TABLE 1. U-Pb SHRIMP DATA OF SAMPLE CR15 FROM THE LA SAL MOUNTAINS MIDDLE LACCOLITH INTRUSION

							Isotope ratios					Ages (Ma)		
Spot		U (ppm)	Th (ppm)	^{206}Pb (ppm)	f206_4 (%)	Th/U	^{207}Pb/^{235}U	±error*	^{206}Pb/^{238}U	±error*	rho	Age	±error*	Disc.† (%)
15.1	*MC*	*1965*	*182*	*6.8*	*0.7*	*0.09*	*0.02740*	*0.00173*	*0.00397*	*0.00024*	*0.68*	*25.5*	*1.5*	*6.9*
10.1	OD	3607	1278	14.0	0.3	0.36	0.02867	0.00054	0.00439	0.00004	0.35	28.3	0.3	1.4
09.1	OD	1336	226	5.1	0.2	0.17	0.02874	0.00081	0.00442	0.00004	0.23	28.4	0.2	1.4
19.1	OD	816	126	3.1	0.0	0.16	0.02889	0.00123	0.00444	0.00012	0.44	28.6	0.8	1.0
16.1	MC	1023	194	3.9	0.6	0.19	0.02915	0.00064	0.00445	0.00007	0.55	28.6	0.4	2.1
17.1	OD	977	160	3.8	0.0	0.17	0.03071	0.00158	0.00446	0.00008	0.25	28.7	0.5	6.5
27.1	OD	1306	341	5.1	0.6	0.27	0.02923	0.00096	0.00447	0.00010	0.51	28.7	0.6	2.0
07.1	OD	1789	110	7.0	0.0	0.06	0.02924	0.00085	0.00450	0.00011	0.58	28.9	0.6	1.4
18.1	OD	1637	325	6.4	0.2	0.20	0.02989	0.00055	0.00450	0.00006	0.52	28.9	0.4	3.3
20.2	OD	1829	545	7.1	0.9	0.31	0.03051	0.00065	0.00449	0.00009	0.67	28.9	0.6	5.2
05.1	OD	1398	339	5.5	1.4	0.25	0.02746	0.00068	0.00451	0.00010	0.65	29.0	0.7	–5.5
02.2	OD	789	149	3.1	0.7	0.19	0.02862	0.00073	0.00452	0.00011	0.67	29.1	0.7	–1.7
12.1	OD	1915	722	7.5	0.6	0.39	0.02845	0.00065	0.00453	0.00007	0.49	29.1	0.4	–2.1
21.1	OD	2144	612	8.4	0.2	0.29	0.02980	0.00080	0.00453	0.00004	0.24	29.1	0.2	2.3
26.1	OD	3450	983	13.8	-0.1	0.29	0.03047	0.00080	0.00454	0.00007	0.40	29.2	0.4	4.3
13.1	OD	1432	400	5.7	0.0	0.29	0.03014	0.00099	0.00456	0.00007	0.35	29.3	0.4	3.0
14.1	OD	2008	424	7.9	0.3	0.22	0.03087	0.00088	0.00455	0.00005	0.29	29.3	0.3	5.2
08.1	OD	1069	176	4.2	–0.4	0.17	0.03048	0.00113	0.00456	0.00006	0.26	29.4	0.4	3.6
24.1	OD	2218	602	8.8	0.5	0.28	0.02841	0.00043	0.00457	0.00005	0.52	29.4	0.3	–3.5
25.1	OD	1873	568	7.4	0.3	0.31	0.02954	0.00085	0.00457	0.00010	0.52	29.4	0.6	0.7
23.1	OD	1602	374	6.4	0.6	0.24	0.02912	0.00123	0.00458	0.00011	0.41	29.5	0.7	–1.4
03.1	OD	1555	456	6.2	0.3	0.30	0.02956	0.00058	0.00460	0.00004	0.35	29.6	0.3	0.0
04.1	OD	2608	799	10.6	–0.1	0.31	0.02922	0.00062	0.00470	0.00005	0.37	30.2	0.3	–3.4
06.1	OD	2427	576	9.9	0.8	0.24	0.02965	0.00060	0.00472	0.00004	0.28	30.4	0.3	–2.4
20.1	*MC*	*308*	*40*	*2.0*	*0.0*	*0.13*	*0.45037*	*0.19779*	*0.00764*	*0.00216*	*0.46*	*49.0*	*13.8*	*87.0*
02.1	XC	193	77	50.0	0.0	0.41	4.20198	0.09481	0.29923	0.00597	0.64	1658.1	18.2	–0.8
01.1	XC	410	108	108.0	0.0	0.27	4.35048	0.05030	0.30403	0.00328	0.67	1692.9	3.8	–0.5
09.2	XC	940	233	231.5	0.0	0.25	4.09743	0.09895	0.28458	0.00623	0.65	1704.3	17.4	2.4
04.2	XC	667	179	180.1	0.0	0.28	4.49357	0.03623	0.31198	0.00197	0.56	1704.9	6.4	–1.2
11.1	XC	723	253	197.6	0.0	0.36	4.56377	0.05877	0.31565	0.00390	0.69	1711.9	1.0	–1.5
22.1	XC	644	210	172.2	0.0	0.33	4.57893	0.05855	0.30909	0.00368	0.67	1756.5	5.4	0.5

Note: Analyses in gray italics are excluded due to a high discordance (>10%) and/or large uncertainties (>5%). Point to point errors, calculated on replicates of the TEMORA standard, are 0.30% for ^{206}Pb/^{238}U and 0.62% for ^{207}Pb/^{206}Pb. Data are uncorrected for common lead. OD—oscillatory domain (magmatic); MC—magmatic core; XC—xenocrystic core; f206_4 denotes the percentage of ^{206}Pb that is common Pb; ^{206}Pb/^{238}Pb ages are used for zircons younger than 1.5 Ga and ^{207}Pb/^{206}Pb ages are used for zircons older than 1.5 Ga.

*All errors are 1σ.

†Discordance is calculated as Disc. (%) = 100 x [1 – (^{206}Pb/^{238}U age/^{207}Pb/^{235}U age)].

ince (Premo and Van Schmus, 1989) and could have provided grains with these ages.

The 22 analyses on oscillatory zoned domains and one remaining analysis on a magmatic core gave ^{206}Pb/^{238}U ages ranging from to 30.4 to 28.3 Ma; the majority of ages are between 29.5 and 28.5 Ma (Fig. 5). The weighted mean ^{206}Pb/^{238}U age is 29.1 ± 0.3 Ma, and this is considered to be the best age estimate for the crystallization age of the intrusion.

AFT Results

The results obtained from the AFT analysis are presented in Table 2 and Figure 6. The AFT ages range from 64.5 ± 3.6 to 16.7 ± 1.3 Ma. With the exception of samples CR05, CR19, and CR20, all ages were significantly younger than depositional ages of the overlying sedimentary rocks. This indicates that a process other than sedimentary burial caused post-Cretaceous thermal annealing

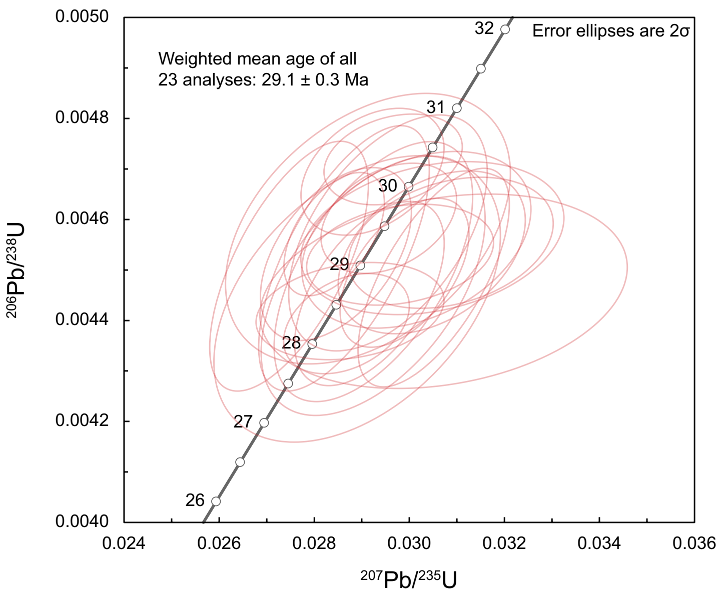

Figure 5. Concordia diagram of the 23 spots located on oscillatory zoned domains and magmatic cores for sample CR15.

in these samples. In the following we discuss the AFT results with respect to four subareas (Fig. 2): the La Sal Mountains, the Unaweep Canyon, the top of the basement of the Uncompahgre Plateau, and the northeastern margin of the plateau (CNM).

La Sal Mountains

Six samples from the La Sal Mountains yielded AFT ages ranging from 32.8 ± 2.5 to 27.5 ± 2.5 Ma. These samples were collected at elevations between 2815 and 3830 m, constituting a vertical profile with sampling intervals of ~200 m. A very steep age-elevation trend is apparent, suggesting fast cooling and little or no thermal influence after crystallization. Confined track length measurements on samples CR11 and CR14 yielded mean track lengths of 13.3 ± 0.67 μm and 13.53 ± 0.27 μm, respectively. Dislocations and other crystal defects are abundant in the samples from the La Sal Mountains, making track counting difficult. The poor sample quality can explain some of the spread in ages. All samples, except for sample CR12 (<5%), passed the χ^2 test. There is no reason to suspect more than one age component in sample CR12, thus the failed χ^2 test is also attributed to poor sample quality. The mean age for all six samples is 29.7 ± 2.1 Ma and this overlaps, within the uncertainties, with the crystallization age of the intrusion.

Unaweep Canyon

Six samples were dated from the Unaweep Canyon. The AFT ages range from 34.9 ± 2.3 to 26.6 ± 2.3 Ma and are similar to the ages obtained from the La Sal Mountains and to eruption ages in the San Juan and West Elk volcanic fields. (e.g., Bove et al., 2001; Garcia, 2011; Lipman and Bachmann, 2015). This suggests that the samples were thermally affected during the late Eocene to Oligocene regional-scale volcanism. The ages are increasing from the southwestern canyon entrance toward the center of the canyon (Unaweep divide) and decrease again toward northeast. This trend is probably an effect of changes in elevation. Length measurements were performed on 4 of the 6 samples, with mean track lengths varying between 10.85 ± 0.93 and 13.14 ± 0.40 μm.

Uncompahgre Plateau

Three samples from outside of Unaweep Canyon, from the top of the basement of the Uncompahgre Plateau, just below the overlying sediments, gave Paleocene ages, showing only a small variation between 63.5 ± 4.0 and 63.0 ± 4.0 Ma. Therefore, the late Eocene to Oligocene thermal event that reset all the samples from within the Unaweep Canyon apparently had little effect on the AFT ages on the top of the Uncompahgre Plateau.

The preserved sedimentary rocks on top of the sampled Precambrian basement are of Late Triassic to Late Cretaceous age (Williams, 1964; Jamison and Stearns, 1982). The early Paleogene AFT ages thus indicate heating during Mesozoic burial and subsequent cooling during Laramide uplift and erosion. None of the samples from the Uncompahgre Plateau passed the χ^2 test, but similar to sample CR12 from the La Sal Mountains, this might be attributed to the relatively poor sample quality in combination with overall high track densities. The mean confined track lengths range from 10.22 ± 0.63 to 12.36 ± 0.21 μm.

CNM

The CNM yielded the youngest ages of 16.7 ± 1.3 and 19.7 ± 1.9 Ma. Sample CR02, with an age of 33.0 ± 2.5 Ma shows similarities to the samples located within the Unaweep Canyon. Length measurements were performed on all three samples, with mean track lengths ranging from 10.40 ± 0.42 to 12.51 ± 0.44 μm.

AHe Results

While all AFT ages from the Unaweep Canyon were reset during late Eocene to Oligocene magmatism, the AFT ages from the top of the basement of the Uncompahgre Plateau seem unaffected, indicating that temperatures here were not high enough to reset the AFT system (70–110 °C). The (U-Th)-He system is sensitive to even lower temperatures (40–70 °C) and thus two samples (CR05 and CR19) were selected for (U-Th)-He analysis, in order to further

TABLE 2. APATITE FISSION-TRACK DATA

Sample number	Elevation (masl)	Global positioning system coordinates		Lithology	Number of grains	Spontaneous track density ($\times 10^5$ cm^{-2})	Induced track density ($\times 10^5$ cm^{-2})	Nd ($\times 10^5$ cm^{-2})	χ^2 probability (%)	Central age (Ma) ± 1σ	U (ppm)	Mean track length ± standard error* (µm)
Colorado National Monument												
CR01	1450	N 39° 07.189′	W 108° 44.745′	migmatitic metasedimentary rock	21	2.983 (190)	42.914 (2733)	20.549 (31964)	94.8	16.7 ± 1.3	31	12.51 ± 0.44 (18)
CR02	1450	N 39° 01.645′	W 108° 38.336′	migmatitic metasedimentary rock	26	4.132 (212)	29.858 (1532)	20.500 (31964)	85.6	33.0 ± 2.5	22	10.40 ± 0.42* (53)
CR03	1550	N 39° 01.638′	W 108° 38.244′	migmatitic metasedimentary rock	21	2.192 (148)	26.911 (1817)	20.431 (31964)	14.9	19.7 ± 1.9	18	11.64 ± 0.52* (23)
Top basement												
CR05	2200	N 38° 44.771′	W 108° 33.463′	granite	27	11.075 (977)	41.828 (3690)	20.313 (31964)	0.02	64.5 ± 2.6	29	12.21 ± 0.20* (100)
CR19	1940	N 38° 56.198′	W 109° 03.431′	gneiss	18	31.469 (660)	112.907 (2368)	19.546 (31964)	0.8	63.5 ± 4.0	85	12.36 ± 0.21* (102)
CR20	1840	N 39° 00.420′	W 108° 56.839′	granite	20	15.992 (761)	57.432 (2733)	19.379 (10669)	0.4	63.0 ± 4.0	44	10.22 ± 0.63 (12)
Unaweep Canyon												
CR04	2015	N 38° 50.782′	W 108° 34.097′	gneiss	25	12.403 (343)	101.397 (2804)	20.372 (31964)	78.7	29.0 ± 1.7	70	12.50 ± 0.33 (26)
CR06	2055	N 38° 45.223′	W 108° 45.610′	granitic gneiss	23	6.636 (403)	44.164 (2682)	20.417 (10669)	9.3	34.9 ± 2.3	31	N.D.
CR07	1995	N 38° 46.261′	W 108° 49.141′	metagabbro	30	15.383 (919)	101.518 (6065)	20.3478 (10669)	27.8	34.8 ± 1.7	72	13.14 ± 0.40* (100)
CR08	1925	N 38° 51.074′	W 108° 32.149′	granite	21	1.755 (136)	13.886 (1076)	20.279 (10669)	75.7	29.1 ± 2.8	9	11.28 ± 0.86* (14)
CR16	1595	N 38° 43.509′	W 108° 54.575′	granite	21	3.818 (184)	32.476 (1565)	19.725 (10669)	22.8	26.6 ± 2.3	23	N.D
CR17	1750	N 38° 45.698′	W 108° 83.966′	granite	23	5.619 (264)	42.972 (2019)	19.656 (10669)	12.6	29.5 ± 2.3	32	10.85 ± 0.93 (9)
La Sal Mountains												
CR10	3620	N 38° 26.497′	W 109° 15.016′	hornblende plagioclase trachyte	13	5.725 (200)	42.391 (1481)	20.209 (10669)	85.0	31.0 ± 2.5	33	N.D.
CR11	3830	N 38° 26.298′	W 109° 13.924′	hornblende plagioclase trachyte	16	7.298 (209)	51.921 (1487)	20.018 (31964)	92.7	32.8 ± 2.5	47	13.23 ± 0.67* (5)
CR12	3430	N 38° 26.325′	W 109° 14.639′	hornblende plagioclase trachyte	18	3.671 (155)	26.575 (1122)	19.959 (31964)	0.7	32.7 ± 4.2	26	N.D.
CR13	3055	N 38° 28.341′	W 109° 16.596′	peralkaline trachyte	11	3.149 (154)	24.642 (1205)	20.002 (10669)	98.3	29.0 ± 2.6	17	N.D.
CR14	2815	N 38° 28.909′	W 109° 16.942′	peralkaline trachyte	24	1.938 (142)	16.269 (1192)	19.782 (31964)	88.1	27.5 ± 2.5	14	13.53 ± 0.27* (39)
CR15	3280	N 38° 26.491′	W 109° 12.961′	hornblende plagioclase trachyte	11	3.738 (87)	27.500 (640)	19.795 (10669)	40.6	30.6 ± 3.7	19	N.D.

Note: masl—meters above sea level; N.D.—not determined. The Uncompahgre Plateau is divided into three parts; the Colorado National Monument, top basement, and the Unaweep Canyon. Spontaneous track densities are measured on the minerals internal surfaces, while the induced and neutron track densities are obtained from mica external detectors. Parentheses show the total number of tracks counted. Ages were calculated by using $\zeta = 227.5 \pm 5.9$ for samples with Nd values of 10669, and $\zeta = 233.5 \pm 9.3$ for samples with Nd values of 31964. Lithology names for the Colorado National Monument correspond to the geological map of Scott et al. (2001); lithology for the La Sal Mountains is consistent with names given by Ross (1998).

*Unit: Samples where californium radiation is applied.

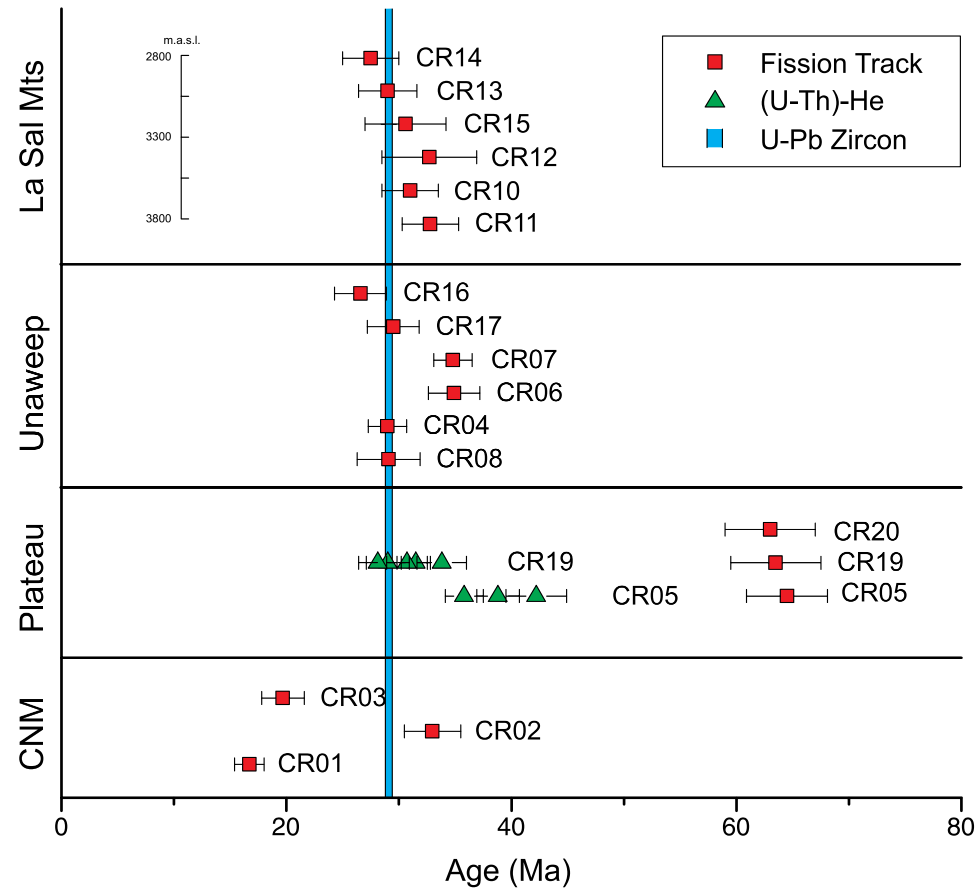

Figure 6. Schematic illustration of the geochronological results with their uncertainties for each dated sample, divided into geographical groups (La Sal Mountains, Unaweep Canyon, top of the basement of the Uncompahgre Plateau and Colorado National Monument, CNM). Samples CR05 and CR19 include apatite (U-Th)-He analyses. Fission track ages are central ages (±1σ) and (U-Th)-He ages (±1σ) are plotted as single grain ages (see Tables 2 and 3). Elevations are given for the La Sal Mountains samples to reflect the vertical profile in this area.

investigate the presence of the late Eocene to Oligocene thermal overprint on top of the Uncompahgre Plateau. Five single apatite grains from sample CR19 yielded ages between 33.8 ± 2.2 and 28.1 ± 1.7 Ma (Table 3; Fig. 4); the mean age is 30.6 ± 2.2 Ma. These ages overlap, within their uncertainties, with the AFT ages from the Unaweep Canyon and the crystallization age of the La Sal Mountains intrusion. This indicates that the late Eocene to Oligocene thermal event is present in the samples from the top of the basement of the Uncompahgre Plateau and that temperatures were high enough to reset (U-Th)-He ages but not AFT ages.

Sample CR05 yielded four slightly older ages ranging from 47.6 ± 2.2 to 35.8 ± 1.7 Ma. The oldest age should be excluded because the apatite contained small inclusions (reported during grain selection), and a higher He re-extract indicates that these might have influenced the He measurement. The mean of the remaining three ages is 38.3 ± 2.3 Ma, indicating that this sample underwent even lower temperatures than sample CR19, which were insufficient to completely reset even the (U-Th)-He system.

Thermal History Modeling

Thermal history models were created by using the HeFTy software (Ketcham, 2005, 2013), with the annealing algorithm by Ketcham et al. (2007) for the AFT data. The (U-Th)-He data were included in the models for the samples CR05 and CR19, calibrated with the kinetic properties of Durango apatite (Farley, 2000). The ending condition for each model was set to 100 good paths. The Uncompahgre Plateau was fully buried by the Western Interior Seaway

TABLE 3. APATITE (U-Th)-He DATA

Sample	He volume* (ncm³)	He 1σ† (%)	238U mass (ng)	238U 1σ† (%)	238U conc.§ (ppm)	232Th mass (ng)	232Th 1σ† (%)	232Th conc.§ (ppm)	Th/U ratio	Sm mass (ng)	Sm 1σ† (%)	Sm conc.§ (ppm)	Ejection correction (Ft)#	Uncorrected He age (Ma)	Ft-Corrected He age (Ma)	1σ** (Ma)	Sample unweighted average†† ±1σ (Ma)	(Ma)
CR05 a1§§	*0.454*	*1.5*	*0.088*	*1.9*	*22.9*	*0.067*	*2.5*	*17.54*	*0.76*	*0.533*	*5.2*	*139*	*0.728*	*34.6*	*47.6*	*2.2*		
CR05 a2	0.193	1.9	0.058	2.0	33.2	0.038	2.6	21.76	0.66	0.187	6.2	108	0.583	23.5	40.2	2.7		
CR05 a3	0.492	1.5	0.123	1.9	35.3	0.075	2.5	21.30	0.60	0.610	4.9	174	0.718	27.9	38.8	1.9		
CR05 a4	0.532	1.5	0.141	1.9	27.9	0.112	2.5	22.26	0.80	0.548	5.2	109	0.715	25.6	35.8	1.7	38.3##	2.3
CR19 a1	0.886	1.4	0.335	1.8	219.3	0.081	2.5	52.88	0.24	0.405	5.4	265	0.606	20.5	33.8	2.2		
CR19 a2	0.814	1.4	0.363	1.8	243.5	0.095	2.5	63.86	0.26	0.388	4.9	260	0.598	17.3	29.0	1.9		
CR19 a3	4.394	1.3	1.397	1.8	246.9	0.399	2.4	70.56	0.29	1.332	4.2	236	0.768	24.2	31.5	1.3		
CR19 a4	0.754	1.4	0.339	1.8	205.9	0.065	2.5	39.28	0.19	0.391	4.8	237	0.620	17.5	28.1	1.7		
CR19 a5	0.625	1.5	0.241	1.8	128.4	0.059	2.5	31.51	0.25	0.454	5.0	242	0.651	20.0	30.7	1.8	30.6	2.2

Note: Analysis in gray italics was excluded (see text).
*Amount of helium is given in ncm (nano-cubic-centimeter), at standard temperature and pressure.
†Uncertainties of helium and the radioactive element contents are given as 1σ, in relative error percent.
§Uncertainties of the radioactive element concentrations (conc.) are ~10% (due to the high uncertainty in the crystal mass estimation).
#Ejection correction (Ft): correction factor for alpha-ejection according to Farley et al. (1996) and Hourigan et al. (2005).
**Uncertainties of the single grain ages are given as 1σ (in Ma) and include both the analytical uncertainties and the estimated uncertainties of Ft.
††Uncertainties of the sample average ages are the standard deviation (1σ).
§§Analysis was excluded (see text).
##Average age based on the analyses CR05 a2–CR05 a4.

throughout Cretaceous time, but might have undergone sedimentation until Paleocene–Eocene time; this is evident from the stratigraphic record of the nearby Book Cliffs (Gualtieri, 1988). Triassic–Cretaceous burial is implemented in the models as a series of boxes that the temperature paths must pass through. These first three boxes (blue boxes in Figs. 7 and 8) are based on the sedimentary record of the Book Cliffs and not determined by the thermochronological data. Since neither the exact timing nor depths are known for the maximum burial, a large box was chosen to allow the models a lot of freedom. The maximum temperatures did not exceed ~200 °C, however, because zircon fission track ages from the area are not reset (Thomson et al., 2012). A large box was also used for the following uplift because timing and the amount of associated cooling were to be determined by the modeling. The timing of reheating during the late Eocene to Oligocene magmatism is well known, but the temperatures reached during this event are not well constrained. Thus this reheating event was implemented as a narrow but high box to allow a lot of freedom in the temperature but not in the timing. The final constraint is the present-day average surface temperature of ~11 °C.

Unaweep Canyon

Unaweep Canyon sample CR07 was chosen for thermal history modeling because it yielded the highest number of tracks. Due to the complete thermal overprint in the late Eocene to Oligocene, the earlier thermal histories have effectively been erased and cannot be constrained by thermochronological data. This is reflected in the wide scatter of pre-Oligocene cooling paths (Fig. 7A). However, constraints can be placed on the late Eocene to Oligocene thermal event and subsequent cooling: The model requires minimum temperatures of ~90 °C during the thermal event. The maximum temperature is poorly defined. Most good-fit paths indicate temperatures between 90 and 110 °C (Fig. 7B); however, paths with acceptable fit can also be found for much higher temperatures. This thermal episode was followed initially by rapid cooling to below 60 °C at ca. 30 Ma, and then a period of slower cooling to ~30 °C at ca. 5 Ma. The model suggests increased cooling rates during the last 5 m.y.

CNM

Length measurements were performed on all three samples from the CNM, but sample CR02 yielded the most confined tracks and was chosen for modeling. Thermal history modeling of this sample reveals late Eocene to Oligocene reheating to temperatures between 80 and 110 °C, similar to the Unaweep Canyon sample (CR07). This thermal event apparently caused complete resetting of the fission track system, and the thermal histories prior to the Oligocene are unconstrained (Figs. 7C, 7D). Contrary to sample CR07, the model indicates relatively slow cooling until ca.10 Ma and 50 °C, followed by rapid cooling to present-day surface temperatures.

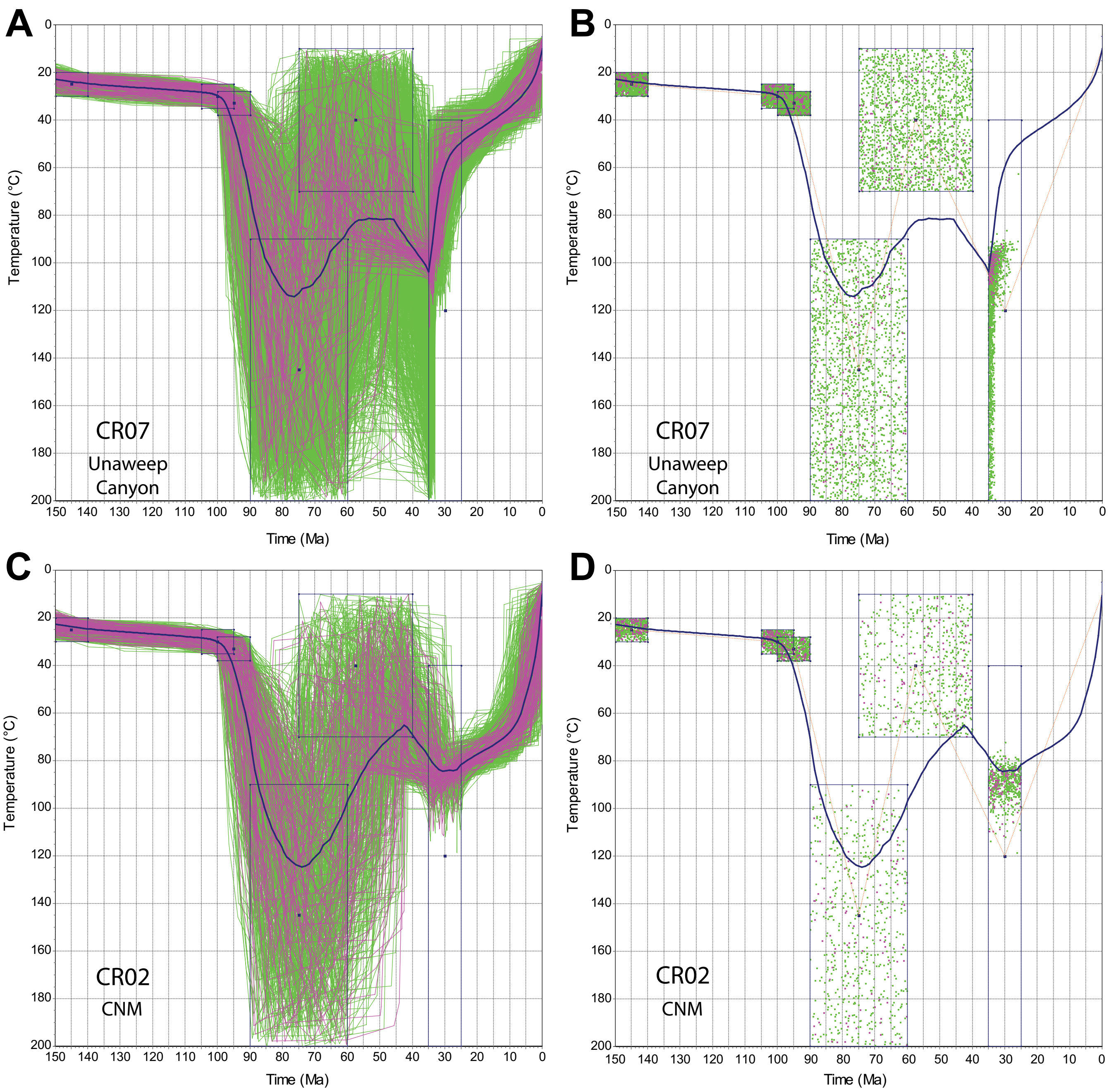

Figure 7. (A–D) Thermal history models for samples CR07 (Unaweep Canyon) and CR02 (Colorado National Monument, CNM), based on apatite fission track data. Good fit paths and nodal points are magenta, and acceptable fit paths and nodal points are green. The blue line is the weighted mean path, and the blue boxes represent the thermal constraints used. First three boxes in the models refer to geological constraints with known stratigraphic ages and temperatures; two large boxes are used to infer the uncertain timing and temperature of sedimentary burial and the subsequent Laramide uplift; one narrow box to allow for reheating during the well-known Late to Oligocene magmatism; last range on the right y-axis is to set the present-day temperature.

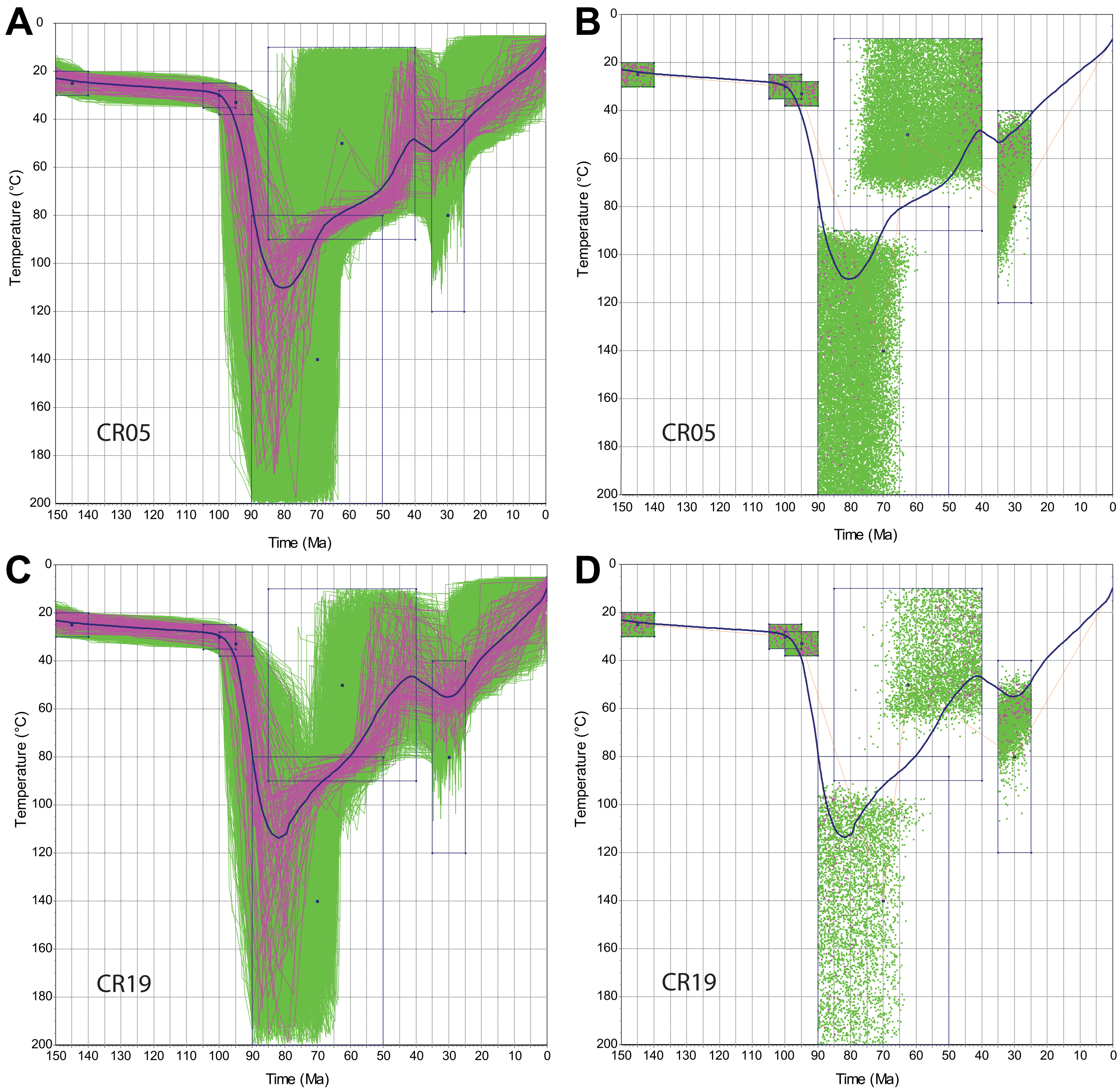

Figure 8. (A–D) Thermal history models for samples CR05 and CR19, based on apatite fission track and apatite (U-Th)-He data. Good fit paths and nodal points are magenta, and acceptable fit paths and nodal points are green. The blue line is the weighted mean path. The blue boxes represent the time-temperature constraints used during modelling. The three small boxes on the left are based on the known burial history of the Uncompahgre Plateau; the paths must pass through these boxes. The larger boxes were used where geological constraints (times, temperatures) were uncertain or unknown and were to be determined by the thermal modelling. The end point at 0 Ma is the present-day temperature.

Uncompahgre Plateau

Thermal history modeling of the Uncompahgre Plateau was performed on samples CR05 and CR19. Both fission track and (U-Th)-He data were included in the thermal history modeling for these samples. Both models (Figs. 8A–8D) suggest maximum burial at ca. 80 Ma, although the timing is not well constrained. The temperature reached at least 90 °C at that time, but might have been significantly higher (Figs. 8B, 8D). The models suggest subsequent cooling to temperatures below 60 °C throughout the Late Cretaceous to Eocene, followed by minor reheating in the early Oligocene to temperatures of ~40–70 °C (CR05) and 50–80 °C (CR19). The samples cooled to present-day temperatures at moderate and relatively constant cooling rates. No significant increase in cooling rates in the last 10 m.y. could be observed.

THERMAL EVOLUTION OF THE UNCOMPAHGRE PLATEAU

Mesozoic Sedimentation and Laramide Uplift

The only samples that did not undergo late Eocene to Oligocene thermal resetting are three samples with Laramide (early Paleocene) cooling ages from the top of the basement of the Uncompahgre Plateau. Thermal history models of these samples reveal rapid sedimentary burial during the Late Cretaceous. Maximum burial depths were reached at ca. 80 Ma, although the timing is not well defined by the modeled time-temperature paths (Figs. 8A, 8C). The temperatures reached during maximum burial are not well constrained, but our models suggest heating to at least 90 °C. Based on present-day temperatures of ~11 °C and a typical thermal gradient of 25–30 °C/km, this corresponds to a section of ~3 km of sediments covering the Uncompahgre Plateau at that time.

The upper Cretaceous sedimentary record for the Uncompahgre Plateau, with alternating sandstones and marine shales, reflects numerous fluctuations in the Western Interior Seaway prior to Laramide uplift (Kauffman, 1977; Cole, 1987; Blakey and Ranney, 2008). The youngest preserved stratigraphic unit on the Uncompahgre Plateau is generally known to be the Dakota Sandstone, but some exposures of marine Mancos Shale can be found on its eastern rim and in the southernmost part of the plateau (Williams, 1964). It is reasonable to believe that younger sediments such as the Mesaverde Group (to 75–70 Ma) found on the nearby Book Cliffs were also deposited on the Uncompahgre Plateau. Based on estimated sediment thicknesses, the total thickness of the preserved Mesozoic section in the Book Cliffs is 2–3 km (Gualtieri, 1988), which is similar to the ~3 km estimated for the Uncompahgre Plateau based on our thermal history modeling.

Late Cretaceous sedimentation was followed by uplift and exhumation during the Late Cretaceous–Paleocene Laramide orogeny. Our thermal models do not provide a precise time for the onset of this event, but suggest that cooling started no later than 65 Ma. This is in general agreement with thermochronological data from the southwestern part of the Colorado Plateau (Naeser et al., 1989; Dumitru et al., 1994; Kelley et al., 2001). These thermochronological data were obtained from the Kaibab uplift area, which has structural similarities (monoclines and reverse faults) to other uplifted segments at the Colorado Plateau, such as the Echo Cliffs, Circle Cliffs, San Rafael Swell, Monument, and Uncompahgre uplift further northeast (e.g., Kelley, 1955; Davis, 1978). The Kaibab and Uncompahgre uplifts are regarded as the most comparable, being the only segments with an exposure of basement rocks at the surface. AHe data from the central Colorado Plateau uplifts, with ages ranging from 44.5 to 11.5 Ma, do not record Laramide exhumation (Stockli et al., 2002). These ages are most likely influenced by the mid-Cenozoic laccolithic intrusions of the Henry, Abajo, and La Sal Mountains.

Late Eocene to Oligocene Magmatism

U-Pb zircon dating of the middle La Sal Mountains laccolith yielded an Oligocene crystallization age of 29.1 ± 0.3 Ma. This generally confirms the previously published U-Pb age of 32 ± 2 Ma (Stern et al., 1965), which was obtained by the borax fusion technique. The La Sal Mountains laccolith is thus one of three large magmatic bodies that intruded the Colorado Plateau in the late Eocene to Oligocene; the other two are located in the Henry and Abajo Mountains. Fission track ages from the La Sal Mountains laccolith (this study; Chew and Donelick, 2012) are virtually identical to the U-Pb zircon crystallization age. The intrusion must therefore have cooled rapidly to temperatures <110 °C (closure temperature of the AFT system; Green et al., 1986), suggesting emplacement at shallow crustal depths. The latter is consistent with the porphyritic texture of the laccolith with a very fine grained groundmass typical of subvolcanic rocks (see Ross, 1998, for description and distribution of igneous rocks).

Late Eocene to Oligocene magmatism had a profound impact on the entire Uncompahgre Plateau. All AFT ages along the Unaweep Canyon and along the northeastern margin of the plateau (CNM) were reset during the late Eocene to Oligocene. AFT samples from the top of the basement of the Uncompahgre Plateau did not undergo late Eocene to Oligocene thermal resetting, but the more temperature-sensitive (U-Th)-He system was affected. AFT data from Thomson et al. (2012) and Aslan et al. (2014) also suggest thermal resetting along the entire Unaweep Canyon, although most of their reported ages are slightly younger (25–20 Ma) than those presented here. AHe data reported by Thomson et al. (2012) for the central and western part of the canyon show a relatively large range of ages from 47 to 17 Ma. However, no analytical details about the (U-Th)-He ages are published, so it is difficult to assess the data quality and thus the reliability of those ages. Combining all three studies, almost all AFT and AHe ages produced to date support complete thermal resetting of both thermochronometers within the Unaweep Canyon and resetting of the AHe ages on the top of the Uncompahgre Plateau basement during the late Eocene to Oligocene. The temperatures inside the canyon must thus have reached the AFT closure temperature (~110 °C; Green et al., 1986), while temperatures at the top of the basement of the plateau must have reached at least the AHe partial retention zone (40–80 °C; Wolf et al., 1996; Stockli et al., 2000). This is consistent with thermal modeling results that indicate Oligocene temperatures of at least 90 °C (possibly much higher) in the Unaweep Canyon, temperatures between 80 and 110 °C in the CNM area, and temperatures between 40 and 80 °C on the top of the basement of the Uncompahgre Plateau. Thomson et al. (2012) presented zircon (U-Th)-He ages that range from completely unreset ages of 309–271 Ma to partially or almost completely reset ages of 81–34 Ma. The closure temperature for the zircon (U-Th)-He system is between ~160 and 200 °C (Reiners et al., 2004). It is therefore possible that the maximum temperatures were variable along the canyon and at least locally reached the zircon (U-Th)-He closure temperature. Zircon fission track ages (309–280 Ma; Thomson et al., 2012) are entirely unaffected by the late Eocene to Oligocene thermal event, placing an upper constraint of ~200 °C (closure temperature of the zircon fission track system ~200–240 °C; Zaun and Wagner, 1985; Hurford, 1986) on maximum temperatures that might have been reached during the late Eocene to Oligocene event.

The thermal resetting has been attributed to an elevated thermal gradient during the late Eocene to Oligocene magmatism. The laccolith intrusion in the nearby La Sal Mountains might have reset low-temperature thermochronometers in the surrounding country rock. Thomson et al. (2012) suggested that a thermal effect from this laccolith can be observed to at least 25 km in all directions. Such a thermal influence from the La Sal Mountains laccolith might explain the thermal resetting of the AFT ages within the southwestern part of the canyon. However, it seems unlikely that this thermal effect extended throughout the northeastern part of the canyon, resetting the AFT system as much as 60 km away from the intrusion. In addition, the effect of thermal resetting seems to be decreasing vertically from the canyon to the top of the plateau rather than horizontally away from the laccolith, as could be expected if the intrusion was the sole heat source. This begs the question whether there could be another intrusive body hidden beneath the Uncompahgre Plateau. Alternatively, considering the abundance of late Eocene to Oligocene magmatism within and around the Colorado Plateau, it seems conceivable that the entire region was characterized by high geothermal gradients at the time, such that subsurface samples even at relatively shallow depth were thermally reset and are now exposed by canyon incision.

The encroachment of late Eocene to Oligocene magmatism onto the Colorado Plateau has led researchers to call for an additional uplift event (e.g., Humphreys et al., 2003; Roy et al., 2009; Liu and Gurnis, 2010; Roberts et al., 2012). A secondary mid-Cenozoic uplift phase has also been recognized by thermochronological studies in the southwestern Colorado Plateau (Flowers et al., 2008; Lee et al., 2013; Karlstrom et al., 2014). However, erosion and rebound estimates from the northern Colorado Plateau imply slow denudation from 30 to 10 Ma (McMillan et al., 2006; Lazear et al., 2013). Our thermal models for the top of the basement of the Uncompahgre Plateau, including AFT and AHe data, show no increased cooling rates after the late Eocene to Oligocene magmatism. No abrupt change in exhumation or uplift is evident from our data.

Neogene: Uplift and Canyon Incision

The youngest AFT ages from the entire Uncompahgre Plateau are two Miocene ages from the CNM, revealing some post-Oligocene exhumation or thermal event along the northeastern plateau margin. Both samples were collected relatively close to the Monument and Fruita Canyon fault systems, and the Precambrian rocks in this area are generally highly fractured; therefore, they might have been partially reset by hydrothermal fluid circulation along the faults. This thermal event might be related to renewed magmatic activity in the area, documented by ca. 10 Ma basaltic lava flows on nearby Grand Mesa (Fig. 3) and other volcanic activity in the region (e.g., Kunk et al., 2002). However, we prefer to interpret these ages as renewed fault activity and/or erosion along the plateau margin in the context of another important event that is only revealed in the thermal history modeling.

Our time-temperature model based on AFT data from the Unaweep Canyon (sample CR07; Figs. 7A, 7D) reveals two cooling phases: one immediately following the late Eocene to Oligocene thermal resetting of the AFT system and a second phase over the past 6 m.y. A late Miocene increase in cooling rates was also observed by Thomson et al. (2012) in samples from the Unaweep Canyon and has been interpreted as canyon incision. Similar patterns of increased cooling rates over the past 6–10 m.y. were recorded by AFT data along the upper Colorado River (Kelley and Blackwell, 1990; Naeser et al., 2002). This aspect was discussed by Soreghan et al. (2015), who connected the fluvial incision acceleration of the upper (10–6 Ma) and the lower (younger than 6 Ma) Colorado River system. Our thermochronological data from the Unaweep Canyon support this theory of a synchronous onset of rapid incision across the entire Colorado Plateau.

The origin and evolution of the modern Colorado River system are unclear (for a summary, see Beard et al., 2011). The key debate involves a shift in drainage course and increased incision through Neogene uplift of the Colorado Plateau and the Rocky Mountains (Leonard, 2002; McMillan et al., 2002, 2006; Aslan et al., 2010; Karlstrom et al., 2012), and/or a base-level fall caused by extension of the neighboring Basin and Range region (Karlstrom et al., 2007, 2008; van Wijk et al., 2010; Pederson and Tressler, 2012; Pederson et al., 2013). Other influencing factors include geomorphic and climatic processes (Molnar and England, 1990; Wobus et al., 2010; Karlstrom et al., 2012; Rosenberg et al., 2014). Our data show that the samples from within the Unaweep Canyon and samples from the northeastern plateau margin underwent rapid late Miocene cooling (from ca. 10 Ma). Samples from the top of the Uncompahgre Plateau basement, however, show moderate and relatively constant cooling rates from the late Eocene to Oligocene thermal event until the present day (this study; Thomson et al., 2012). Thus a late Miocene tectonic event caused rapid cooling in the Unaweep Canyon and rapid cooling as well as fault activity along the northeastern plateau margin, but had no major effect on the plateau (Figs. 9A–9D). A late Miocene–Pliocene uplift of the Uncompahgre Plateau would explain not only the increased cooling rates within the canyon, but also those along the northeastern margin of the plateau (Fig. 9E). Erosion would be focused in

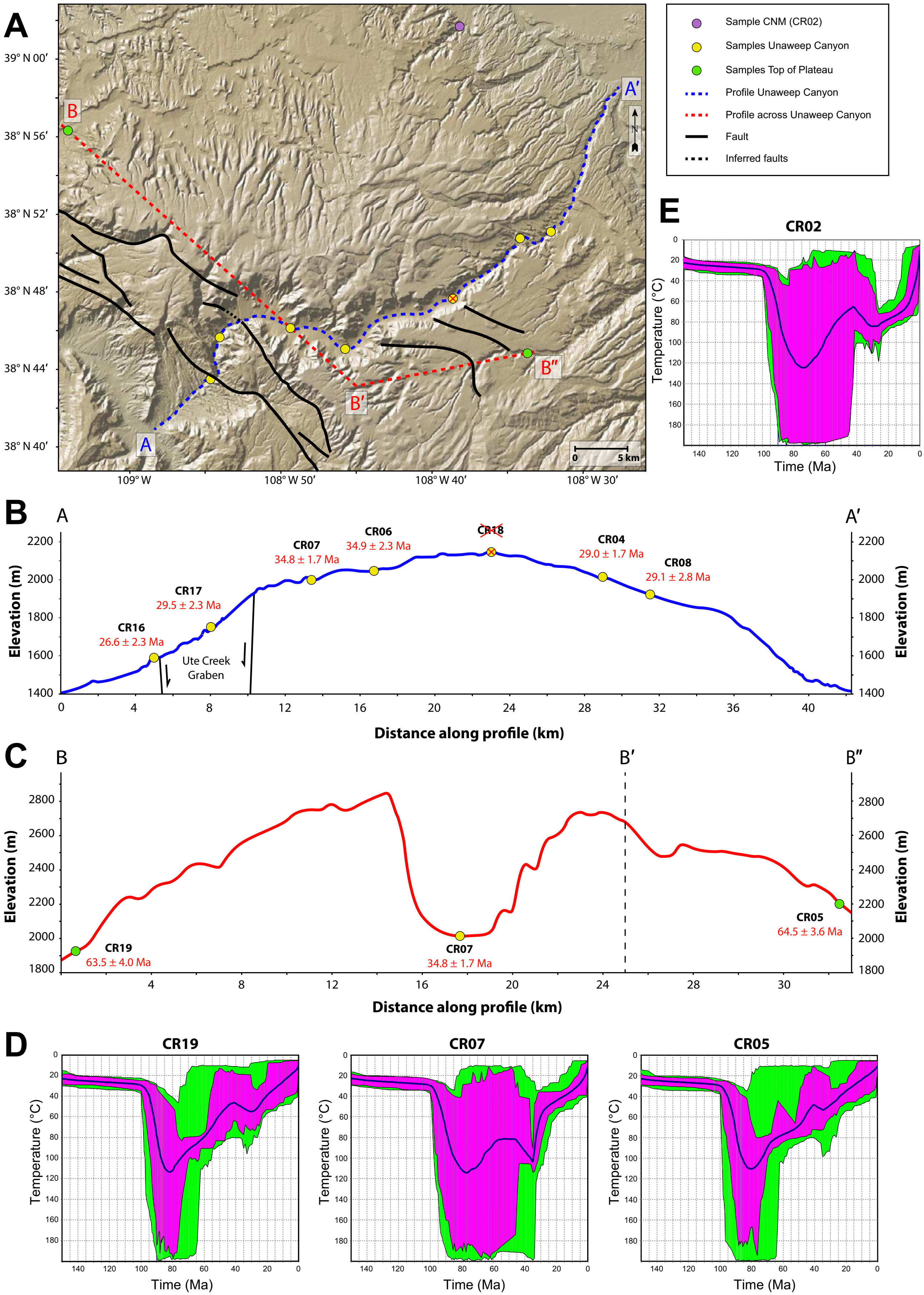

Figure 9. (A) Topographic map of the Unaweep Canyon showing samples from this study along with profiles B and C and adjacent faults. (B) Profile along the Unaweep Canyon valley floor showing how the apatite fission track (AFT) ages are distributed with respect to distance and elevation. (C) Profile across the canyon, illustrating the large age difference for the relatively young sample CR07 (within the canyon), in contrast to the older samples, CR19 and CR05 (outside the canyon), at nearly identical elevations. (D) Thermal history models for the three samples in profile C. (E) Thermal history model for sample CR02 within the Colorado National Monument (CNM).

the canyons and along the plateau margins, while the sediments on the top of the plateau are being more slowly eroded. A Pliocene uplift of the Uncompahgre Plateau area has previously been suggested (e.g., Sinnock, 1981; Scott et al., 2002; Aslan et al., 2008, 2010), even though structural evidence for this is scarce. With evidence for increased incision rates across the region in the past 10 m.y., our new thermochronological data support that large parts of the Colorado Plateau underwent uplift associated with exhumation and canyon incision in late Miocene–Pliocene time.

CONCLUSIONS

AFT data from the top of the Uncompahgre Plateau basement suggest progressive Mesozoic heating through sedimentary burial to ~3 km depth in the Late Cretaceous (assuming a thermal gradient of 30 °C/km). Our thermochronological study does not provide a precise timing for the Laramide uplift, but indicates that cooling started no later than 65 Ma. This coincides with other thermochronological studies on the Colorado Plateau.

Secondary ion mass spectrometry U-Pb zircon dating provides a crystallization age of 29.1 ± 0.3 Ma for the middle La Sal Mountains laccolith. All AFT ages along the Unaweep Canyon and along the northeastern margin of the plateau have been reset during this magmatic event. The thermal gradient seems to decrease upward from the Unaweep Canyon toward the top of the basement of the plateau, suggesting a heat source from below rather than the La Sal Mountains laccolith to the west. Regional elevated temperatures in the late Eocene to Oligocene or an additional intrusive body under the plateau might explain this pattern.

Our thermal models from both the Unaweep Canyon and the CNM suggest a rapid cooling event over the past 5–10 m.y., which we interpret as increased erosion in the canyon and along the plateau margins caused by Miocene–Pliocene uplift of the Uncompahgre Plateau. Accelerated Miocene–Pliocene canyon incision was recognized by several researchers across large parts of the Colorado Plateau and has been linked to either regional Neogene uplift or a base-level fall and/or climatic factors.

ACKNOWLEDGMENTS

This work is based on a master of science project that was financially supported by the University of Bergen. We thank I. Dunkl (University of Göttingen) for help with the (U-Th)-He analyses, F. Bea and P. Montero (University of Granada) for help with the U-Pb zircon analyses, and R.M. Russo, S. Kelley, A. Cavosie, R.M. Kirkham, and an anonymous reviewer for critically reading an earlier version of the manuscript. Rønnevik thanks F. Kohlmann for help with the fission track method and P. Quam and J. Quam for their hospitality during field work.

REFERENCES CITED

Armstrong, R.L., 1969, K-Ar dating of laccolithic centers of the Colorado Plateau and vicinity: Geological Society of America Bulletin, v. 80, p. 2081–2086, doi:10.1130/0016-7606(1969)80[2081:KDOLCO]2.0.CO;2.

Aslan, A., et al., 2008, River incision histories of the Black Canyon of the Gunnison and Unaweep Canyon: Interplay between late Cenozoic tectonism, climate change, and drainage integration in the western Rocky Mountains, *in* Raynolds, R.G., ed., Roaming the Rocky Mountains and Environs: Geological Field Trips: Geological Society of America Field Guide 10, p. 175–202, doi:10.1130/2008.fld010(09).

Aslan, A., Karlstrom, K.E., Crossey, L.J., Kelley, S., Cole, R., Lazear, G., and Darling, A., 2010, Late Cenozoic evolution of the Colorado Rockies: Evidence for Neogene uplift and drainage integration, *in* Morgan, L.A., and Quane, S.L., eds., Through the Generations: Geologic and Anthropogenic Field Excursions in the Rocky Mountains from Modern to Ancient: Geological Society of America Field Guide 18, p. 21–54, doi:10.1130/2010.0018(02).

Aslan, A., Hood, W.C., Karlstrom, K.E., Kirby, E., Granger, D.E., Kelley, S., Crow, R., Donahue, M.S., Polyak, V., and Asmerom, Y., 2014, Abandonment of Unaweep Canyon (1.4–0.8 Ma), western Colorado: Effects of stream capture and anomalously rapid Pleistocene river incision: Geosphere, v. 10, p. 428–446, doi:10.1130/GES00986.1.

Beard, L.S., Karlstrom, K.E., Young, R.A., and Billingsley, G.H., eds., 2011, CREvolution 2—Origin and Evolution of the Colorado River System, Workshop Abstracts: U.S. Geological Survey Open-File Report 2011–1210, 300 p., https://pubs.usgs.gov/of/2011/1210/.

Black, L.P., Kamo, S.L., Allen, C.M., Aleinikoff, J.A., Davis, D.W., Korsch, J.R., and Foudolis, C., 2003, TEMORA 1: A new zircon standard for Phanerozoic U-Pb geochronology: Chemical Geology, v. 200, p. 155–170, doi:10.1016/S0009-2541(03)00165-7.

Blakey, R., and Ranney, W., 2008, Ancient Landscapes of the Colorado Plateau: Grand Canyon, Arizona, Grand Canyon Association, 156 p.

Bove, D.J., Hon, K., Budding, K.E., Slack, J.F., Snee, L.W., and Yeoman, R.A., 2001, Geochronology and Geology of Late Oligocene Through Miocene Volcanism and Mineralization in the Western San Juan Mountains, Colorado: U.S. Geological Survey Professional Paper 1642, 30 p.

Case, J.E., 1991, Geologic Map of the Northwestern Part of the Uncompahgre Uplift, Grand County, Utah, and Mesa County, Colorado, with Emphasis on Proterozoic rocks: U.S. Geological Survey Miscellaneous Investigations Series Map I-2088, scale 1:24,000.

Cashion, W.B., 1973, Geologic and Structure Map of the Grand Junction Quadrangle, Colorado and Utah: U.S. Geological Survey Miscellaneous Geologic Investigations Map I-736, scale 1:250,000.

Cater, F.W., 1966, Age of the Uncompahgre Uplift and Unaweep Canyon, West-Central Colorado: U.S. Geological Survey Professional Paper 550-C, p. C86–C92.

Cater, F.W., 1970, Geology of the Salt Anticline Region in Southwestern Colorado: U.S. Geological Survey Professional Paper 637, 84 p.

Cather, S.M., Chapin, C.E., and Kelley, S.A., 2012, Diachronous episodes of Cenozoic erosion in southwestern North America and their relationship to surface uplift, paleoclimate, paleodrainage, and paleoaltimetry: Geosphere, v. 8, p. 1177–1206, doi:10.1130/GES00801.1.

Chew, D.M., and Donelick, R.A., 2012, Combined apatite fission track and U-Pb dating by LA-ICP-MS and its application in apatite provenance analysis, *in* Sylvester, P., ed., Quantitative Mineralogy and Microanalysis of Sediments and Sedimentary Rocks: Mineralogical Association of Canada Short Course 42, p. 219–247.

Claoue-Long, J.C., Compston, W., Roberts, J., and Fanning, C.M., 1995, Two Carboniferous ages: A comparison of SHRIMP zircon dating with conventional zircon ages and $^{40}Ar/^{39}Ar$ analysis, *in* Berggren, W.A., et al., eds., Geochronology, Time Scales, and Global Stratigraphic Correlation: SEPM (Society for Sedimentary Geology) Special Publication 54, p. 3–21, doi:10.2110/pec.95.04.0003.

Cole, R.D., 1987, Cretaceous Rocks of the Dinosaur Triangle, *in* Averett, W.R., ed., Dinosaur Triangle Paleontology Field Trip: Grand Junction, Colorado, Grand Junction Geological Society, p. 21–35.

Cole, R.D., and Young, R.G., 1983, Evidence for glaciation in Unaweep Canyon, Mesa County, Colorado, *in* Averett, W.R., ed., Northern Paradox Basin–Uncompahgre Uplift: Grand Junction, Colorado, Grand Junction Geological Society, p. 73–80.

Davis, G.H., 1978, Monocline fold pattern of the Colorado Plateau, *in* Matthews, V.I., ed., Laramide Folding Associated with Basement Block Faulting in the Western United States: Geological Society of America Memoir 151, p. 215–234, doi:10.1130/MEM151-p215.

Donelick, R.A., O'Sullivan, P.B., and Ketcham, R.A., 2005, Apatite fission-track analysis: Reviews in Mineralogy and Geochemistry, v. 58, p. 49–94, doi:10.2138/rmg.2005.58.3.

Dumitru, T.A., 1993, A new computer-automated microscope stage system for fission-track analysis: Nuclear Tracks and Radiation Measurements, v. 21, p. 575–580, doi:10.1016/1359-0189(93)90198-I.

Dumitru, T.A., Duddy, I.R., and Green, P.F., 1994, Mesozoic–Cenozoic burial, uplift, and erosion history of the west-central Colorado Plateau: Geology, v. 22, p. 499–502, doi:10.1130/0091-7613(1994)022<0499:MCBUAE>2.3.CO;2.
Dunkl, I., 2002, Trackkey: A Windows program for calculation and graphical presentation of fission track data: Computers & Geosciences, v. 28, p. 3–12, doi:10.1016/S0098-3004(01)00024-3.
Farley, K.A., 2000, Helium diffusion from apatite: General behavior as illustrated by Durango fluorapatite: Journal of Geophysical Research, v. 105, no. B2, p. 2903–2914, doi:10.1029/1999JB900348.
Farley, K.A., Wolf, R.A., and Silver, L.T., 1996, The effects of long alpha-stopping distances on (U-Th)/He ages: Geochimica et Cosmochimica Acta, v. 60, p. 4223–4229, doi:10.1016/S0016-7037(96)00193-7.
Flowers, R.M., Wernicke, B.P., and Farley, K.A., 2008, Unroofing, incision, and uplift history of the southwestern Colorado Plateau from apatite (U-Th)/He thermochronometry: Geological Society of America Bulletin, v. 120, p. 571–587, doi:10.1130/B26231.1.
Gannett, H., 1882, The Unaweep Canon: Popular Scientific Monthly, v. 20, p. 781–786.
Garcia, R.V., 2011, Cenozoic Intrusive and Exhumation History of the West Elk Mountains, Southwestern Colorado [M.S. thesis]: Socorro, New Mexico Institute of Mining and Technology, 200 p.
Green, P.F., Duddy, I.R., Gleadow, A.J.W., Tingate, P.R., and Laslett, G.M., 1986, Thermal annealing of fission tracks in apatite: 1. A qualitative description: Chemical Geology, v. 59, p. 237–253, doi:10.1016/0168-9622(86)90074-6.
Gualtieri, J., 1988, Geologic Map of the Westwater 30′ × 60′ Quadrangle, Grand and Uintah Counties, Utah and Garfield and Mesa Counties, Colorado: U.S. Geological Survey Miscellaneous Geologic Investigations Map I-1765, scale 1:100,000.
Hoffman, M., Stockli, D.F., Kelley, S.A., Pederson, J., and Lee, J., 2011, Mio-Pliocene erosional exhumation of the central Colorado Plateau, eastern Utah—New insights from apatite (U-Th)/He thermochronometry, *in* Beard, L.S., et al., eds., CREvolution 2—Origin and Evolution of the Colorado River System, Workshop Abstracts: U.S. Geological Survey Open-File Report 2011-1210, p. 132–136.
Hood, W.C., 2009, An exhumed late Paleozoic canyon in the Rocky Mountains: A discussion: Journal of Geology, v. 117, p. 210–214, doi:10.1086/595789.
Hood, W.C., 2011, Unaweep Canyon—Which River Ran Through It?: The Mountain Geologist, v. 48, no. 2, p. 45–57.
Hood, W.C., Cole, R.D., and Aslan, A., 2009, Anomalous cold in the Pangaean tropics: Comment: Geology, v. 37, p. e192, doi:10.1130/G30035C.1.
Hood, W.C., Aslan, A., and Betton, C., 2014, Aftermath of a stream capture: Cactus Park lake spillover and the origin of East Creek, Uncompahgre Plateau, western Colorado: Geosphere, v. 10, p. 447–461, doi:10.1130/GES00970.1.
Hourigan, J.K., Reiners, P.W., and Brandon, M.T., 2005, U/Th zonation dependent alpha ejection in (U-Th)/He chronometry: Geochimica et Cosmochimica Acta, v. 69, p. 3349–3365, doi:10.1016/j.gca.2005.01.024.
Humphreys, E., Hessler, E., Dueker, K., Farmer, G.L., Erslev, E., and Atwater, T., 2003, How Laramide-age hydration of North American lithosphere by the Farallon slab controlled subsequent activity in the western United States: International Geology Review, v. 45, p. 575–595, doi:10.2747/0020-6814.45.7.575.
Hunt, C.B., 1956, Cenozoic Geology of the Colorado Plateau: U.S. Geological Survey Professional Paper 279, 99 p.
Hurford, A.J., 1986, Cooling and uplift patterns in the Lepontine Alps, south central Switzerland and an age of vertical movement on the Insubric fault line: Contributions to Mineralogy and Petrology, v. 92, p. 413–427, doi:10.1007/BF00374424.
Hurford, A.J., and Green, P.F., 1983, The zeta age calibration of fission-track dating: Isotope Geoscience, v. 1, p. 285–317, doi:10.1016/S0009-2541(83)80026-6.
Jamison, W.R., 1989, Fault-fracture strain in Wingate Sandstone: Journal of Structural Geology, v. 11, p. 959–974, doi:10.1016/0191-8141(89)90047-3.
Jamison, W.R., and Stearns, D.W., 1982, Tectonic deformation of Windgate Sandstone, Colorado National Monument: American Association of Petroleum Geologists Bulletin, v. 66, p. 2584–2608.
Kaplan, S., Soreghan, G., Sweet, D., and Blum, M., 2005, The history of the ancestral Gunnison River through western Unaweep Canyon and Gateway (Colorado): Geological Society of America Abstracts with Programs, v. 37, no. 6, p. 34.
Karlstrom, K.E., Crow, R.S., Peters, L., McIntosh, W., Raucci, J., Crossey, L.J., Umhoefer, P., and Dunbar, N., 2007, $^{40}Ar/^{39}Ar$ and field studies of Quaternary basalts in Grand Canyon and model for carving Grand Canyon: Quantifying the interaction of river incision and normal faulting across the western edge of the Colorado Plateau: Geological Society of America Bulletin, v. 119, p. 1283–1312, doi:10.1130/0016-7606(2007)119[1283:AAFSOQ]2.0.CO;2.
Karlstrom, K.E., Crow, R., Crossey, L.J., Coblentz, D., and Van Wijk, J.W., 2008, Model for tectonically driven incision of the younger than 6 Ma Grand Canyon: Geology, v. 36, p. 835–838, doi:10.1130/G25032A.1.
Karlstrom, K.E., et al., 2012, Mantle-driven dynamic uplift of the Rocky Mountains and Colorado Plateau and its surface response: Toward a unified hypothesis: Lithosphere, v. 4, p. 3–22, doi:10.1130/L150.1.
Karlstrom, K.E., et al., 2014, Formation of the Grand Canyon 5 to 6 million years ago through integration of older palaeocanyons: Nature Geoscience, v. 7, p. 239–244, doi:10.1038/ngeo2065.
Kauffman, E.G., 1977, Geological and biological overview: Western Interior Cretaceous basin: The Mountain Geologist, v. 14, p. 75–99.
Kelley, S.A., and Blackwell, D.D., 1990, Thermal history of the Multi-Well Experiment (MWX) site, Piceance Creek Basin, northwestern Colorado, derived from fission-track analysis: Nuclear Tracks and Radiation Measurements, v. 17, p. 331–337, doi:10.1016/1359-0189(90)90055-3.
Kelley, S.A., Chapin, C.E., and Karlstrom, K.E., 2001, Laramide cooling histories of Grand Canyon, Arizona, and the Front Range, Colorado, determined from apatite fission-track thermochronology, *in* Young, R.A., and Spamer, E.E., eds., Colorado River Origin and Evolution: Grand Canyon, Arizona, Grand Canyon Association, p. 37–42.
Kelley, V.C., 1955, Monoclines of the Colorado Plateau: Geological Society of America Bulletin, v. 66, p. 789–804, doi:10.1130/0016-7606(1955)66[789:MOTCP]2.0.CO;2.
Ketcham, R.A., 2005, Forward and inverse modeling of low-temperature thermochronometry data: Reviews in Mineralogy and Geochemistry, v. 58, p. 275–314, doi:10.2138/rmg.2005.58.11.
Ketcham, R.A., and Donelick, R.A., 2013, HeFTy Version 1.8.0, User Manual: Department of Geological Sciences, University of Texas at Austin, 72 p.
Ketcham, R.A., Donelick, R.A., Barbarand, J.K., and Hurford, A.J., 2007, Improved measurement of fission-track annealing in apatite using c-axis projection: American Mineralogist, v. 92, p. 789–798, doi:10.2138/am.2007.2280.
Kirkham, R.M., and Rogers, W.P., 1981, Earthquake potential in Colorado: Colorado Geological Survey Bulletin, v. 43, p. 171.
Kunk, M.J., Budahn, J.R., Unruh, D.M., Stanley, J.O., Kirkham, R.M., Bryant, B., Scott, R.B., Lidke, D.J., and Streufert, R.K., 2002, $^{40}Ar/^{39}Ar$ ages of late Cenozoic volcanic rocks within and around the Carbondale and Eagle collapse centers, Colorado: Constraints on the timing of evaporite-related collapse and incision of the Colorado River, *in* Kirkham, R.M., et al., eds., Late Cenozoic Evaporite Tectonism and Volcanism in West-Central Colorado: Geological Society of America Special Paper 366, p. 213–234, doi:10.1130/0-8137-2366-3.213.
Lazear, G., Karlstrom, K., Aslan, A., and Kelley, S., 2013, Denudation and flexural isostatic response of the Colorado Plateau and southern Rocky Mountains region since 10 Ma: Geosphere, v. 9, p. 792–814, doi:10.1130/GES00836.1.
Lee, J.P., Stockli, D.F., Kelley, S.A., Pederson, J.L., Karlstrom, K.E., and Ehlers, T.A., 2013, New thermochronometric constraints on the Tertiary landscape evolution of the central and eastern Grand Canyon, Arizona: Geosphere, v. 9, p. 216–228, doi:10.1130/GES00842.1.
Leonard, E.M., 2002, Geomorphic and tectonic forcing of late Cenozoic warping of the Colorado piedmont: Geology, v. 30, p. 595–598, doi:10.1130/0091-7613(2002)030<0595:GATFOL>2.0.CO;2.
Lipman, P.W., and Bachmann, O., 2015, Ignimbrites to batholiths: Integrating perspectives from geological, geophysical, and geochronological data: Geosphere, v. 11, p. 705–743, doi:10.1130/GES01091.1.
Liu, L., and Gurnis, M., 2010, Dynamic subsidence and uplift of the Colorado Plateau: Geology, v. 38, p. 663–666, doi:10.1130/G30624.1.
Lohman, S.W., 1961, Abandonment of Unaweep Canyon, Mesa County, Colorado, by Capture of the Colorado and Gunnison Rivers: U.S. Geological Survey Professional Paper 424, p. B144–B146.
Lohman, S.W., 1965, Geology and Artesian Water Supply, Grand Junction Area, Colorado: U.S. Geological Survey Professional Paper 451, 157 p.
Lohman, S.W., 1981, Ancient drainage changes in and south of Unaweep Canyon, southwestern Colorado, *in* Epis, R.C., and Callender, J.F., eds., Western Slope (Western Colorado and Eastern Utah): New Mexico Geological Society Guidebook 32, p. 137–143.

McCalpin, J.P., 2004, Neotectonics of the Roubideau Creek Fault, Uncompahgre Plateau, Colorado; A Preliminary Assessment: Crestone, Colorado, GEO-HAZ Consulting, 41 p.

McCalpin, J.P., 2006, Neotectonics of Quaternary Faults Q20, Q22 and Q23 in the Central Uncompahgre Plateau, Colorado: Crestone, Colorado, GEO-HAZ Consulting, 65 p.

McMillan, M.E., Angevine, C.L., and Heller, P.L., 2002, Postdepositional tilt of the Miocene–Pliocene Ogallala Group on the western Great Plains: Evidence of late Cenozoic uplift of the Rocky Mountains: Geology, v. 30, p. 63–66, doi:10.1130/0091-7613(2002)030<0063:PTOTMP>2.0.CO;2.

McMillan, M.E., Heller, P.L., and Wing, S.L., 2006, History and causes of post-Laramide relief in the Rocky Mountain orogenic plateau: Geological Society of America Bulletin, v. 118, p. 393–405, doi:10.1130/B25712.1.

Molnar, P., and England, P., 1990, Late Cenozoic uplift of mountain ranges and global climate change: Chicken or egg?: Nature, v. 346, p. 29–34, doi:10.1038/346029a0.

Murray, K.E., Reiners, P.W., and Thomson, S.N., 2016, Rapid Pliocene–Pleistocene erosion of the central Colorado Plateau documented by apatite thermochronology from the Henry Mountains: Geology, v. 44, p. 483–486, doi:10.1130/G37733.1.

Naeser, C.W., Duddy, I.R., Elston, D.P., Dumitru, T.A., and Green, P.F., 1989, Fission-track dating: Ages for Cambrian strata and Laramide and post-middle Eocene cooling events from the Grand Canyon, Arizona, *in* Elston, D.P., et al., eds., Geology of the Grand Canyon, Northern Arizona (With Colorado River Guides): Lee Ferry to Pierce Ferry, Arizona: Washington, D.C., American Geophysical Union, p. 139–144, doi:10.1029/FT115p0139.

Naeser, C.W., Bryant, B., Kunk, M.J., Kellogg, K., Donelick, R.A., and Perry, W.J., Jr., 2002, Tertiary cooling and tectonic history of the White River uplift, Gore Range, and western Front Range, central Colorado: Evidence from fission-track and $^{39}Ar/^{40}Ar$ ages, *in* Kirkham, R.M., et al., eds., Late Cenozoic Evaporite Tectonism and Volcanism in West-Central Colorado: Geological Society of America Special Paper 366, p. 31–54, doi:10.1130/0-8137-2366-3.31.

Nelson, S.T., and Davidson, J.P., 1998, The petrogenesis of the Colorado Plateau laccoliths and their relationship to regional magmatism, *in* Friedman, J.D., and Huffman, A.C., Jr., ed., Laccolith Complexes of Southeastern Utah: Tectonic Control and Time of Emplacement–Workshop Proceedings: U.S. Geological Survey Bulletin 2158, p. 86–98.

Nelson, S.T., Davidson, J.P., and Sullivan, K.R., 1992, New age determinations of central Colorado Plateau laccoliths, Utah: Recognizing disturbed K-Ar systematics and re-evaluating tectonomagmatic relationships: Geological Society of America Bulletin, v. 104, p. 1547–1560, doi:10.1130/0016-7606(1992)104<1547:NADOCC>2.3.CO;2.

Oesleby, T.W., 1983, Geophysical measurement of valley fill thickness in Unaweep Canyon, west-central Colorado, *in* Averett, W.R., ed., Northern Paradox Basin–Uncompahgre Uplift: Grand Junction, Colorado, Grand Junction Geological Society, p. 71.

Oesleby, T.W., 2005, Thick sediment fill in Unaweep Canyon: Implications for the history of the Uncompahgre uplift, western Colorado: Geological Society of America Abstracts with Programs, v. 37, no. 6, p. 16.

Peale, A.C., 1877, Geological report on the Grand River district, *in* U.S. Geological and Geographical Survey of the Territories, Ninth Annual Report: Washington, D.C., U.S. Government Printing Office, p. 31–101.

Pederson, J.L., and Tressler, C., 2012, Colorado River long-profile metrics, knickzones and their meaning: Earth and Planetary Science Letters, v. 345, p. 171–179, doi:10.1016/j.epsl.2012.06.047.

Pederson, J.L., Cragun, W.S., Hidy, A.J., Rittenour, T.M., and Gosse, J.C., 2013, Colorado River chronostratigraphy at Lee's Ferry, Arizona, and the Colorado Plateau bull's-eye of incision: Geology, v. 41, p. 427–430, doi:10.1130/G34051.1.

Premo, W.R., and Van Schmus, W.R., 1989, Zircon geochronology of Precambrian rocks in southeastern Wyoming and northern Colorado, *in* Grambling, J.A., and Tewksbury, B.J., eds., Proterozoic Geology of the Southern Rocky Mountains: Geological Society of America Special Paper 235, p. 13–32, doi:10.1130/SPE235-p13.

Reiners, P.W., Spell, T.L., Nicolescu, S., and Zanetti, K.A., 2004, Zircon (U-Th)/He thermochronometry: He diffusion and comparisons with $^{40}Ar/^{39}Ar$ dating: Geochimica et Cosmochimica Acta, v. 68, p. 1857–1887, doi:10.1016/j.gca.2003.10.021.

Roberts, G.G., White, N.J., Martin-Brandis, G.L., and Crosby, A.G., 2012, An uplift history of the Colorado Plateau and its surroundings from inverse modeling of longitudinal river profiles: Tectonics, v. 31, TC4022, doi:10.1029/2012TC003107.

Rosenberg, R., Kirby, E., Aslan, A., Karlstrom, E., Heizler, M., and Ouimet, W., 2014, Late Miocene erosion and evolution of topography along the western slope of the Colorado Rockies: Geosphere, v. 10, p. 641–663, doi:10.1130/GES00989.1.

Ross, M.L., 1998, Geology of the Tertiary intrusive centers of the La Sal Mountains, Utah—Influence of preexisting structural features on emplacement and morphology, *in* Friedman, J.D., and Huffman, A.C., Jr., ed., Laccolith Complexes of Southeastern Utah: Tectonic Control and Time of Emplacement—Workshop Proceedings: U.S. Geological Survey Bulletin 2158, p. 61–83.

Roy, M., Jordan, T.H., and Pederson, J., 2009, Colorado Plateau magmatism and uplift by warming of heterogeneous lithosphere: Nature, v. 459, p. 978–982, doi:10.1038/nature08052.

Scott, R.B., Harding, A.E., Hood, W.C., Cole, R.D., Livaccari, R.F., Johnson, J.B., Shroba, R.R., and Dickerson, R.P., 2001, Geologic Map of Colorado National Monument and Adjacent Areas, Mesa County, Colorado: U.S. Geological Survey Geologic Investigations Series I-2740, 40 p., scale 1:24,000.

Scott, R.B., Steven, T.A., Betton, C.W., Cole, R.D., Aslan, A., and Hood, W.C., 2002, Evidence for late Cenozoic uplift on the Uncompahgre Plateau, northeastern Colorado Plateau: Geological Society of America Abstracts with Programs, v. 34, no. 6, p. 322.

Shawe, C.A., and Karlstrom, K.E., 1999, The Yavapai-Mazatzal crustal boundary in the southern Rocky Mountains: Rocky Mountain Geology, v. 34, p. 37–52, doi:10.2113/34.1.37.

Sinnock, S., 1981, Pleistocene drainage changes in Uncompahgre Plateau–Grand Valley region of western Colorado, including formation and abandonment of Unaweep Canyon; a hypothesis, *in* Epis, R.C., and Callender, J.F., eds., Western Slope (Western Colorado and Eastern Utah): New Mexico Geological Society Guidebook 32, p. 127–136.

Soreghan, G.S., Sweet, D.E., Marra, K.R., Eble, C.F., Soreghan, M.J., Elmore, R.D., Kaplan, S.A., and Blum, M.D., 2007, An exhumed late Paleozoic canyon in the Rocky Mountains: Journal of Geology, v. 115, p. 473–481, doi:10.1086/518075.

Soreghan, G.S., Soreghan, M.J., Poulsen, C.J., Young, R.A., Eble, C.F., Sweet, D.E., and Davogustto, O.C., 2008, Anomalous cold in the Pangean tropics: Geology, v. 36, p. 659–662, doi:10.1130/G24822A.1.

Soreghan, G.S., Soreghan, M.J., Poulsen, C.J., Young, R.A., Eble, C.F., Sweet, D., and Davogustto, O.C., 2009a, Anomalous cold in the Pangean tropics: Reply: Geology, v. 37, p. e193–e194, doi:10.1130/G30148Y.1.

Soreghan, G.S., Sweet, D.E., Marra, K.R., Eble, C.F., Soreghan, M.J., Elmore, R.D., Kaplan, S.A., and Blum, M.D., 2009b, An exhumed late Paleozoic canyon in the Rocky Mountains: Reply: Journal of Geology, v. 117, p. 215–220, doi:10.1086/595788.

Soreghan, G.S., Sweet, D.E., and Heavens, N.G., 2014, Upland glaciation in tropical Pangaea: Geologic evidence and implications for late Paleozoic climate modeling: Journal of Geology, v. 122, p. 137–163, doi:10.1086/675255.

Soreghan, G.S., Sweet, D.E., Thomson, S.N., Kaplan, S.A., Marra, K.R., Balco, G., and Eccles, T.M., 2015, Geology of Unaweep Canyon and its role in the drainage evolution of the northern Colorado Plateau: Geosphere, v. 11, p. 320–341, doi:10.1130/GES01112.1.

Stern, T.W., Newell, M.F., Kistler, R.W., and Shawe, D.R., 1965, Zircon uranium-lead and thorium-lead ages and mineral potassium-argon ages of La Sal Mountains rocks, Utah: Journal of Geophysical Research, v. 70, p. 1503–1507, doi:10.1029/JZ070i006p01503.

Stockli, D.F., Farley, K.A., and Dumitru, T.A., 2000, Calibration of the apatite (U-Th)/He thermochronometer on an exhumed fault block, White Mountains, California: Geology, v. 28, p. 983–986, doi:10.1130/0091-7613(2000)28<983:COTAHT>2.0.CO;2.

Stockli, D.F., Bump, A.P., Davis, G., and Farley, K.A., 2002, Preliminary (U-Th)/He thermochronological constraints on timing and magnitude of Tertiary denudation of the Colorado Plateau, Utah: Geological Society of America Abstract with Programs, v. 34, no. 6, p. 321.

Sullivan, K.R., Kowallis, B.J., and Mehnert, H.H., 1991, Isotopic ages of igneous intrusions in southeastern Utah: Evidence for a mid-Cenozoic Reno–San Juan magmatic zone: Brigham Young University Geology Studies, v. 37, p. 139–144.

Thomson, S.N., Soreghan, L.S., and Eccles, T.M., 2012, Elevated Cenozoic geothermal gradients and later post-6 Ma incision of the Uncompahgre Plateau and Unaweep Canyon (western Colorado) revealed by low temperature thermochronology: Geological Society of America Abstracts with Programs, v. 44, no. 6, p. 18.

Trudgill, B.D., 2011, Evolution of salt structures in the northern Paradox Basin: Controls on evaporite deposition, salt wall growth and supra-salt stratigraphic architecture: Basin Research, v. 23, p. 208–238, doi:10.1111/j.1365-2117.2010.00478.x.

van Wijk, J.W., Baldridge, W.S., van Hunen, J., Goes, S., Aster, R., Goblentz, D.D., Grand, S.P., and Ni, J., 2010, Small-scale convection at the edge of the Colorado Plateau: Implications for

topography, magmatism, and evolution of Proterozoic lithosphere: Geology, v. 38, p. 611–614, doi:10.1130/G31031.1.
Whitmeyer, S.J., and Karlstrom, K.E., 2007, Tectonic model for the Proterozoic growth of North America: Geosphere, v. 3, p. 220–259, doi:10.1130/GES00055.1.
Williams, I.S., 1998, U-Th-Pb geochronology by ion microprobe, *in* McKibben, M.A., et al., eds., Applications of Microanalytical Techniques to Understanding Mineralizing Processes: Reviews in Economic Geology Volume 7, p. 1–35.
Williams, I.S., and Claesson, S., 1987, Isotopic evidence for the Precambrian provenance and Caledonian metamorphism of high grade paragneisses from the Seve Nappes, Scandinavian Caledonides. II: Ion microprobe zircon U-Th-Pb: Contributions to Mineralogy and Petrology, v. 97, p. 205–217, doi:10.1007/BF00371240.
Williams, I.S., and Hergt, J.M., 2000, U-Pb dating of Tasmanian dolerites: A cautionary tale of SHRIMP analysis of high-U zircon, *in* Woodhead, J.D., et al., eds., Beyond 2000: New Frontiers in Isotope Geoscience: Abstracts and Proceedings: Mulgrave, Australia, Eastern Press, p. 185–188.
Williams, P., 1964, Geology, Structure, and Uranium Deposits of the Moab Quadrangle, Colorado and Utah: U.S. Geological Survey Miscellaneous Geologic Investigations IMAP 360, scale 1:250,000.
Wobus, C.W., Tucker, G.E., and Anderson, R.S., 2010, Does climate change create distinctive patterns of landscape incision: Journal of Geophysical Research, v. 115, F04008, doi:10.1029/2009JF001562.
Wolf, R.A., Farley, K.A., and Silver, L.T., 1996, Helium diffusion and low-temperature thermochronometry of apatite: Geochimica et Cosmochimica Acta, v. 60, p. 4231–4240, doi:10.1016/S0016-7037(96)00192-5.
Zaun, P.E., and Wagner, G.A., 1985, Fission-track stability in zircons under geological conditions: Nuclear Tracks, v. 10, p. 303–307.